Distribution of Iron–Manganese Concretions in Relation to Seismostratigraphy in the Gulf of Finland

Master's Thesis

Student: Hannah Mikenberg
Student ID: 242228LARM
Supervisors: Atko Heinsalu, TalTech, Senior Researcher, PhD
Sten Suuroja, Geological Survey of Estonia, PhD
Curriculum: Earth Systems and Geotechnology (LARM18/24)

Tallinn 2026

Author's Declaration

Kinnitan, et olen koostanud antud lõputöö iseseisvalt ning seda ei ole kellegi teise poolt varem kaitsmisele esitatud. Kõik töö koostamisel kasutatud teiste autorite tööd, olulised seisukohad, kirjandusallikatest ja mujalt pärinevad andmed on töös viidatud.

Autor: Hannah Mikenberg
25.05.2026

Töö vastab magistritööle esitatavatele nõuetele.
Juhendaja: Atko Heinsalu
25.05.2026

Table of Contents

Distribution of Iron–Manganese Concretions in Relation to Seismostratigraphy in the Gulf of Finland

Abstract

Iron–manganese (Fe–Mn) concretions are widespread on the seafloor of the Gulf of Finland, where they commonly occur together with pockmarks, microbial mats, and erosional seabed features. Despite decades of research and their environmental and economic significance, the geological controls governing their distribution and association with pockmarks as well as fluid seepage remain insufficiently understood. This thesis investigates the spatial distribution of Fe–Mn concretions in four study areas in the Estonian sector of the Gulf of Finland and evaluates their relationship with seabed geomorphology, seismostratigraphy, pockmarks, microbial mats, and possible fluid migration pathways.

The study is based on an integrated interpretation of multibeam bathymetry, backscatter data, seismoacoustic profiling data, sediment cores, and remotely operated vehicle observations acquired during collaborative marine surveys conducted by the Geological Survey of Estonia, the Estonian Transport Administration, and partner institutions between 2022 and 2025. In total, approximately 645 km of chirp sub-bottom profiles and 158 km of boomer seismic profiles were interpreted. Historical sediment core data and Fe–Mn concretion occurrence records were also incorporated into the interpretation. Seven seismoacoustic units (SU1–SU7) were identified and tentatively correlated with the regional geological succession of the Gulf of Finland.

The results show that, within the investigated study areas, Fe–Mn concretions are preferentially associated with elevated and erosional seabed features, characterised by thin or discontinuous sediment cover, and the exposure or near-surface occurrence of older geological units. Concretion-bearing environments are closely linked to glaciolacustrine varved clays deposited during the Baltic Ice Lake stage. A clear spatial association between Fe–Mn concretions and pockmarks was observed in all study areas.

The study suggests that the distribution and preservation of Fe–Mn concretions are controlled by the interaction of seabed geomorphology, sediment stratigraphy, bottom-current erosion, low sedimentation rates, and localised fluid seepage beneath low-permeability glaciolacustrine clays. The results further indicate that fluid migration is controlled by a combination of fractured crystalline basement, local sedimentary units, permeability contrasts, and seabed geomorphology rather than by a single regional aquifer system. Localised seepage and redox-controlled processes therefore appear to play an important role in Fe–Mn concretion formation and preservation within the study areas.

This study provides a basis for future research integrating geophysical, geochemical, porewater, microbiological, and isotopic methods together with deep sediment coring to better constrain fluid origin and the processes controlling Fe–Mn concretion formation in the Baltic Sea.

Soome lahe raua-mangaani konkretsioonide leviku seos merepõhja geoloogilise ehitusega

Lühikokkuvõte

Raua–mangaani (Fe–Mn) konkretsioonid on Soome lahes laialt levinud. Konkretsioonide leviku seaduspärasused ja kujunemist kontrollivad mehhanismid ei ole siiski siiani täielikult selged. Käesolevas magistritöös uuriti Fe–Mn konkretsioonide levikut neljal eelnevalt kaardistatud uuringualal Soome lahes ning hinnati nende esinemise seoseid merepõhja reljeefi, geoloogilise ehituse, lekkimislehtrite, settepinna mikroobsete mattide ja põhjavee liikumisega.

Lõputöö põhineb aastatel 2022–2025 Eesti Geoloogiateenistuse, Transpordiameti ja koostööpartnerite läbi viidud mereekspeditsioonide käigus kogutud seismoakustiliste mõõdistamiste (lehviksonar, chirp- ja boomer-tüüpi põhjaprofilaatorid), puursüdamike ning kaugjuhitavate allveerobotite andmete integreeritud tõlgendamisel. Ühtekokku interpreteeriti ligikaudu 645 km chirp-profiile ja 158 km boomer-profiile. Uuringus kasutati ka varasemaid Soome lahe puursüdamike ning Fe–Mn konkretsioonide proovide andmeid. Uuringualadel liigestati seismoakustiliste profiilide põhjal seitse seismostratigraafilist üksust: kristalne aluskord, Ediacara settekivimid või vanemad kvaternaari setted, viimase jäätumise moreen, Balti jääjärve viirsavid, Joldiamere/Antsülusjärve homogeensed savid, Litoriinamere setted ja Limneamere meremudad.

Lõputööst selgub, et uuringualadel mõjutavad Fe–Mn konkretsioonide levikut merepõhja geomorfoloogia, geoloogiline ehitus, põhjahoovuste põhjustatud erosioon, madal settimiskiirus ning vettpidavate hilisjääaja viirsavide all toimuv põhjavee ja/või gaaside liikumine. Uuritud aladel paiknevad Fe–Mn konkretsioonid tihti merepõhja kõrgendikel ja erosioonialadel, kus viirsavikiht on õhuke või puudub ning vanemad geoloogilised üksused paiknevad merepõhja lähedal. Neid kivimeid/setteid kattev vettpidav viirsavikiht on kõrgendikel osaliselt erodeerunud, kuid mujal merepõhja akumulatsioonialadel levib ühtlaselt umbes 10 m paksuse kihina. Merepõhja kõrgematel aladel paiknevad lekkimislehtrid on paarikümne kuni paarisaja meetrise läbimõõduga ja kuni paari meetri sügavused kraatrilaadsed nõod, mis on kujunenud põhjavee ja/või gaaside liikumisel pudedates setendites ning nende läbimurdmisel läbi vettpidavate viirsavide merepõhjani. Kõigil uuringualadel on Fe–Mn konkretsioonid seotud lekkimislehtritega. Lekkimislehtrite, settepinna mikroobsete mattide ja Fe–Mn konkretsioonide koosesinemine annab alust arvata, et selliseid keskkondi mõjutavad lokaalne põhjavee ja/või gaaside leke ning sette ja vee piirpinnal aset leidvate redokspotentsiaali muutustega seotud biogeokeemilised protsessid.

Käesolev uurimistöö loob aluse edasisteks kompleksseteks meregeoloogilisteks uuringuteks (geofüüsika, geokeemia, mikrobioloogia ja isotoopmeetodid) ja sügavpuurimise läbiviimiseks, mis aitaksid paremini selgitada Läänemere Fe–Mn konkretsioonide kujunemist ja nende leviku seaduspärasusi kontrollivaid protsesse.

List of Figures

List of Tables

List of Abbreviations

Fe–Mn – iron–manganese

SGD – submarine groundwater discharge

ROV – remotely operated vehicle

GIS – geographic information system

R/V – research vessel

CTD – conductivity, temperature, depth

MBES – multibeam echosounders

DTM – digital terrain model

SU – seismoacoustic unit

NW–SE – northwest–southeast

b.s.l. – below sea level

1. Introduction

Iron–manganese (Fe–Mn) concretion fields occur throughout the world's oceans and on continental shelves, including the Baltic Sea. These biogeochemical mineral deposits can host economically valuable elements and provide habitats for benthic ecosystems (Wasiljeff et al., 2025b). Their potential economic significance has also motivated geological investigations and environmental assessments of concretion-bearing areas in the eastern Gulf of Finland (Zhamoida et al., 2017). The relatively rapid growth of shallow-marine Fe–Mn concretions in the Gulf of Finland additionally makes them valuable archives of past environmental conditions (Wasiljeff et al., 2025a). At the same time, the Baltic Sea is increasingly affected by eutrophication and pollution, which frequently results in seafloor deoxygenation (Zillén et al., 2008).

However, under anoxic conditions, microbial dissolution of Fe–Mn concretions may release phosphorus into bottom waters and potentially enhance eutrophication in the Gulf of Finland. Fe–Mn concretions contain more than ten times as much phosphorus as typical seabed sediments. In oxygen-depleted environments, their dissolution may therefore act as an internal phosphorus source, further aggravating eutrophication in the Baltic Sea. It remains unclear whether Fe–Mn concretions function primarily as natural phosphorus sinks or whether they may act as a delayed source of nutrient release, potentially worsening the environmental state of the Baltic Sea (Yli-Hemminki et al., 2016).

Fe–Mn concretions are widely distributed across the floor of the Baltic Sea, particularly in the Gulf of Finland, where reported growth rates range from approximately 0.01 to 0.03 mm yr^{-1} (Shulga et al., 2025). They are especially abundant in the eastern part of the Gulf of Finland (Zhamoida et al., 2017). Their formation occurs in a complex setting governed by hydrodynamic and geochemical conditions, sedimentation rates, and microbial activity. In the Baltic Sea, estuarine circulation, strong water-column stratification, high biological productivity, and eutrophication create dynamic redox conditions that are critical for Fe–Mn concretion development (Shulga et al., 2025).

The seafloor of the eastern Gulf of Finland is covered by Quaternary sediments, including deposits from the last glaciation and younger Holocene clays formed during the Yoldia Sea and the Ancylus Lake stages, as well as brackish-water muds from the Litorina Sea and Limnea Sea stages. The lower part of the Quaternary sequence consists of glacial till that is locally exposed but generally overlain by glaciolacustrine clays. These clays are varved in the lower sections and become more homogeneous upwards, forming widespread seafloor deposits commonly overlain by a thin layer of reworked mixed sediments (Suuroja et al., 2016).

The distribution and morphology of Fe–Mn concretions in the Gulf of Finland are closely linked to seafloor topography and sediment type. They are commonly associated with Ancylus Lake clays and glaciolacustrine varved clays (Zhamoida et al., 2017). In shelf seas such as the Baltic Sea, Fe–Mn concretions typically form in well-oxygenated seafloor areas with low sedimentation rates and limited organic matter input. Different concretion morphologies are commonly associated with different seabed substrates and depositional environments (Wasiljeff et al., 2025b). Accordingly, they are rarely associated with Litorina Sea sediments or modern organic-rich sea muds and generally occur within a relatively narrow depth range near the edges of mud-dominated areas (Zhamoida et al., 2017).

Previous research by the author examined the relationship between Fe–Mn concretions and seabed pockmarks in the Mohni area of the Gulf of Finland (Mikenberg, 2024). The present study represents an expanded continuation of this work and aims to investigate the distribution of concretions in selected study areas of the Gulf of Finland and to evaluate their relationship to seabed geomorphology, geological structure, pockmarks, and microbial mats. By integrating additional study areas, seismoacoustic interpretation, sedimentological data, seabed geomorphological analysis, and sub-bottom profiling data, this study seeks to improve understanding of the processes controlling concretion formation and pockmark development in this glacially influenced marine environment. This thesis addresses the following research questions within the investigated study areas:

1) What controls the spatial distribution of Fe–Mn concretions in relation to seabed geomorphology?
2) Which seismoacoustic units are most commonly associated with Fe–Mn concretion occurrence?
3) To what extent are Fe–Mn concretions associated with seabed pockmarks, and what does this reveal about fluid flow dynamics at the seafloor?

2. Geology of the Baltic Sea and the Gulf of Finland

The Baltic Sea is a shallow, semi-enclosed sea with a mean depth of about 54 m. It is connected to the Atlantic Ocean through the Danish Straits and its brackish character results from limited exchange with the ocean combined with substantial freshwater input from rivers and precipitation. The average salinity is about 7‰ (Leppäranta & Myrberg, 2009), but surface salinity ranges from about 1‰ in the north to 6–8‰ in the central Baltic Sea (Björck, 1995). Near major river mouths, such as the Neva River, salinity is even lower. Water renewal is slow, taking on average roughly 50 years, and strong stratification limits vertical mixing (Leppäranta & Myrberg, 2009).

The Baltic Sea is strongly stratified by salinity (halocline) and temperature (thermocline). A permanent halocline at depths of 50–80 m separates low-salinity surface water from denser, saltier bottom water, while a seasonal thermocline develops at 10–25 m during summer. As a result, oxygen deficiency and even anoxia are common near the seafloor, particularly in deeper basin areas (Leppäranta & Myrberg, 2009). The Gulf of Finland is the easternmost sub-basin of the Baltic Sea. It is bordered by Finland to the north, Estonia to the south, and Russia to the east. The gulf covers an area of about 29,500 km^2 and has an average depth of 37 m. It becomes progressively shallower towards the east, and deep-water renewal occurs only under specific meteorological conditions, mainly during autumn and winter (Leppäranta & Myrberg, 2009).

The Baltic Sea has a long and complex geological history (Harff et al., 2011). It is an old structural depression cut into the Precambrian crystalline bedrock of northern Europe. Tectonically, the basin spans several major geological provinces (Figure 1). The northern part is underlain by the Baltic or Fennoscandian Shield, composed mainly of Precambrian rocks. Farther south, the basin overlies the East European Platform, where the crystalline basement is covered mainly by sedimentary rocks ranging from the Neoproterozoic to the Palaeozoic in age, and is overlain by Quaternary sediments. The southwestern boundary is defined by the Teisseyre-Tornquist Zone, which separates the East European Platform from the West European Palaeozoic Platform (Uścinowicz, 2014).

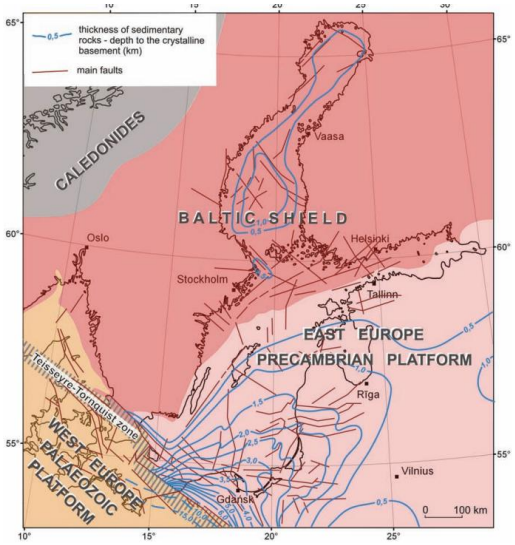

Figure 1. Major tectonic features of the Baltic Sea region (after Uścinowicz, 2014).

Geologically, the Gulf of Finland lies at the boundary between the Fennoscandian Shield and the East European Platform. The northern side is underlain by Precambrian crystalline rocks, whereas on the southern side the crystalline basement is covered by sedimentary rocks of Ediacaran to Middle Ordovician age (ca. 635–460 Ma) (Vallius et al., 2022). Due to a gentle southward dip of the basement, the sedimentary layers form a monoclinal structure with a slope of about 2–4 m km^{-1}. Outcrops of the sedimentary cover generally follow the modern coastline (Figure 2) (Suuroja et al., 2016).

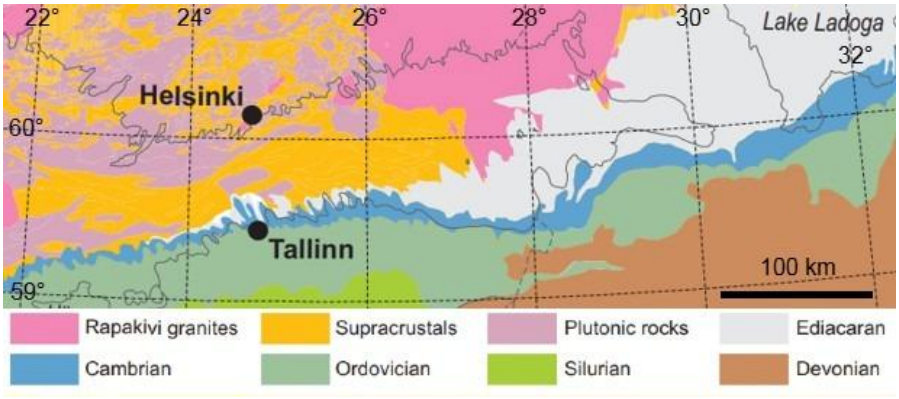

Figure 2. Bedrock geology of the Gulf of Finland region (modified from Vallius et al., 2022).

Because the Baltic Sea basin lies at high northern latitudes, its geological development has been strongly influenced by Quaternary glaciations. During repeated glacial advances and retreats, large parts of the basin were covered by ice sheets. Each glaciation was followed by deglaciation, which caused differential postglacial isostatic uplift. Thus, both sedimentation and basin evolution have been controlled by tectonic setting and repeated glacial-interglacial cycles (Andrén et al., 2011). Prior to the formation of the Baltic Sea, the region was shaped by large river systems, notably the Eridanos River, which existed from the Miocene to the Early Pleistocene and transported sediments southward from the Baltic Shield. Its deposits extend from Poland to the North Sea region (Rhebergen, 2009).

During the Eemian Interglacial (ca. 130,000–115,000 years ago; Marine Isotope Stage 5e), the region was covered by a marine basin connecting the North Sea with the Barents Sea, while large parts of the Fennoscandian Shield remained above sea level (Andrén et al., 2011). Sea levels were higher than present, and marine sediments were deposited across the basin. Many of these deposits were later eroded or buried during the Weichselian glaciation (Gibbard & Knudsen, 2025). Eemian sediments occur in the eastern Baltic region but are often fragmented and deformed due to later glacial activity (Kadastik et al., 2003). In the Gulf of Finland region, Eemian marine deposits have been identified on several islands, including Prangli, Aksi, Malusi, Rammu, Põhja-Uhtju, and Väike Tütarsaar (Kiipli et al., 1993).

The Weichselian glaciation (ca. 115,000–11,500 years ago) reached its maximum extent around 26,000–20,000 years ago. The ice sheet extended south of the present-day Baltic Sea, and its thickness in the central accumulation area near the northern Gulf of Bothnia reached up to 3.5 km. As large amounts of water were stored in continental ice sheets, global sea level was approximately 130–140 m lower than today (Tuuling et al., 2011).

Early Weichselian conditions in northern Estonia were likely still ice-free, and no glacial deposits from this period have been identified. Instead, continental sediments, such as those of the Kelnase unit, formed during this time and are described as spatially limited and not widely distributed (Suuroja et al., 2002). Chronological data indicate that Estonia remained mainly ice-free during much of the Middle Weichselian, although a possible glaciation phase between ca. 68,000–44,000 years ago has been proposed (Lasberg, 2012). Middle Weichselian interstadial sediments from the Voka section in northeastern Estonia consist of laminated sands and clays deposited in a freshwater basin. These deposits, dated to approximately 39,000–31,000 BP (Marine Isotope Stage 3), reflect changing palaeoenvironmental conditions, with pollen data indicating alternating tundra, forest-tundra, and colder steppe-like environments during the interstadial period (Molodkov et al., 2007).

During the Late Weichselian glaciation, the Gulf of Finland region was covered by the Fennoscandian Ice Sheet (Lasberg, 2012). One of the most common surface sediment units in the Gulf of Finland is the Late Weichselian till (Järva Formation), a grey to dark grey, fine-grained, clay-rich glacial deposit typically 4–5 m thick, although locally thinner or absent. The underlying bedrock often shows step-like relief with elevation differences of up to 20 m, which is also seen in overlying sediments such as Baltic Ice Lake varved clays (Lutt & Raukas, 1993). The till is overlain by glaciolacustrine rhythmites, postglacial clays, and brackish-water muds, although their thickness and composition vary locally (Virtasalo et al., 2014a).

When the Weichselian ice sheet retreated, the Baltic Ice Lake formed, which existed from about 16,000 to 11,700 years ago (Figure 3). Initially, it developed as a glaciolacustrine basin in the southwestern Baltic (Rosentau et al., 2017). Meltwater input led to the deposition of varved sediments composed of alternating silty and clayey layers. Near the ice margin, varved clays dominated, while more distal areas accumulated non-laminated glacial clays (Björck, 1995). Sedimentation was glaciolacustrine, and the biological productivity remained very low due to cold, turbid, and nutrient-poor conditions (Andrén et al., 2011).

In the Gulf of Finland, varved clays are commonly exposed at depths of 50–70 m but may be buried in deeper areas or eroded in shallow zones. At the end of the Younger Dryas (ca. 11,700 years ago), rapid drainage through the Billingen area in Sweden lowered the Baltic Ice Lake by about 25 m, exposing coastal areas, and triggering erosion and sediment redistribution (Rosentau et al., 2017). A thin silt layer associated with this event is preserved in some areas (Lutt & Raukas, 1993). Sediment instability during this drainage event led to deformation, slumping, and debris-flow deposits (Hyttinen et al., 2011).

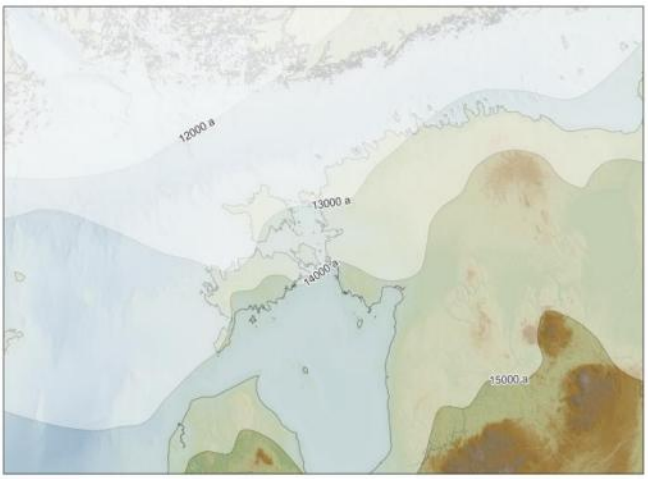

Figure 3. Retreat pattern of the last continental ice sheet in Estonia (based on Hughes et al., 2016).

The next stage was the Yoldia Sea, which corresponded to the onset of the Holocene (Hang et al., 2020). Between approximately 11,700 and 10,700 years ago, the basin had a narrow connection to the ocean across south-central Sweden, and water levels were in equilibrium with the ocean (Heinsalu, 2001). The Yoldia Sea comprised three phases: initial and final freshwater phases and a short brackish-water phase between 11,300 and 11,200 years ago (Heinsalu & Veski, 2007). Yoldia Sea sediments consist mainly of homogeneous or weakly laminated grey silty clays with limited organic content. Thin layers containing black iron monosulphides are associated with the brief brackish-water phase (Lepland et al., 1999; Heinsalu et al., 2000). In the Gulf of Finland, these sediments lie unconformably on Baltic Ice Lake deposits and are typically up to 1 m thick (Suuroja et al., 2016).

Rapid glacio-isostatic land uplift subsequently closed the marine connection, initiating the Ancylus Lake stage (ca. 10,700–9,800 years ago). Ancylus Lake was dammed by an uplifting threshold and meltwater discharge from the retreating ice sheet, until a transgression peaked around 10,200 years ago (Ojala et al., 2005). Ancylus Lake sediments are mainly homogeneous bluish-grey clays with occasional sulphide staining (Winterhalter, 1992). Their structure suggests weak water column stratification, generally oxic bottom conditions, and active bioturbation (Virtasalo et al., 2007). The black sulphide features are interpreted as post-depositional effects (Sternbeck & Sohlenius, 1997). In the Gulf of Finland, these sediments reach thicknesses up to 4–6 m but are not widely exposed at the modern seafloor (Suuroja et al., 2016).

The transition to brackish-water conditions marks the Initial Litorina Sea (ca. 9,800–8,500 years ago), followed by the more saline Litorina Sea, and later the Limnea (Post-Litorina) Sea from about 4,500 years ago (Rosentau et al., 2017). Litorina Sea sediments are typically fine-grained clays and organic-rich muds with abundant brackish-water microfossil assemblages (Andrén et al., 2011). Oxygen conditions at the seafloor varied, with micro-laminated sediments forming under anoxic conditions and bioturbated sediments forming during periods of improved ventilation (Winterhalter, 1992).

In the Gulf of Finland, the Litorina and Limnea Sea sediments are limited and mainly found in deeper areas east of Vaindloo Island (>50 m depth) (Suuroja et al., 2016). The transition from lacustrine to brackish-water sediments is marked by a regional erosional surface associated with the Litorina Sea

transgression (Virtasalo et al., 2016). Furthermore, regional geological mapping indicates that Ancylus Lake deposits are largely absent east of Vaindloo Island, occurring mainly as small, isolated patches. Since Yoldia and Ancylus deposits are often mapped together in the Gulf of Finland, this implies that both units have a very limited distribution in this easternmost part of the basin (Suuroja et al., 2016).

The modern seabed of the Gulf of Finland consists of a mosaic of sediment types. Fine-grained muds accumulate in depositional basins, particularly in the central and southern parts, whereas shallower areas are dominated by coarser sediments or exposed bedrock (Figure 4). Approximately 25% of the gulf is covered by actively accumulating Holocene mud (Vallius et al., 2017). Sedimentation rates are generally below 1 cm yr^{-1} but may reach up to 3 cm yr^{-1} in sheltered coastal depositional basins (Vallius et al., 2022).

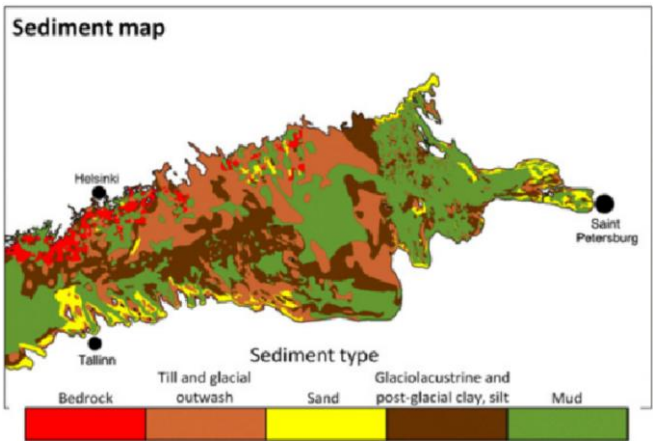

Figure 4. Distribution of surface sediments in the Gulf of Finland (modified from Virtasalo et al., 2014b).

Since the Gulf of Finland has a highly dynamic seabed, storm-driven bottom currents frequently remove the thin Holocene mud layer, exposing older deposits. This results in strong spatial variability in sediment types and makes the seabed highly susceptible to erosion and sediment redistribution (Virtasalo et al., 2014b). Strong bottom-current activity and episodic sediment resuspension are typical characteristics of the Gulf of Finland (Rasmus et al., 2015).

2.1. Iron–manganese Concretions

Fe–Mn concretions are small, rounded, layered mineral formations that develop at the interface between seafloor sediments and overlying water. They occur in a variety of environments, including deep oceans (Hein et al., 2020), brackish-water seas like the Baltic Sea (Majamäki et al., 2025), and freshwater lakes (Riikoja, 1936). Their distribution is closely linked to seafloor topography and sediment type (Zhamoida et al., 2017), and in the Gulf of Finland, they typically form on fine-grained clays and silts (Majamäki et al., 2025).

Large areas of the Gulf of Finland seafloor are covered by Fe–Mn concretions, which are characterised by relatively high phosphorus and manganese contents (Lutt & Raukas, 1993). They are particularly abundant in the eastern part of the gulf (Figure 5), where they occur at moderate depths on gently

sloping clay surfaces that often border modern organic-rich mud accumulation basins. Concretions commonly occur near the margins of these basins and may be partially buried beneath soft sediments (Vallius et al., 2017). Many concretion-bearing slopes are associated with elevated glacial landforms. In the central Gulf of Finland, such seabed morphological features occur near small islands (Suuroja et al., 2016).

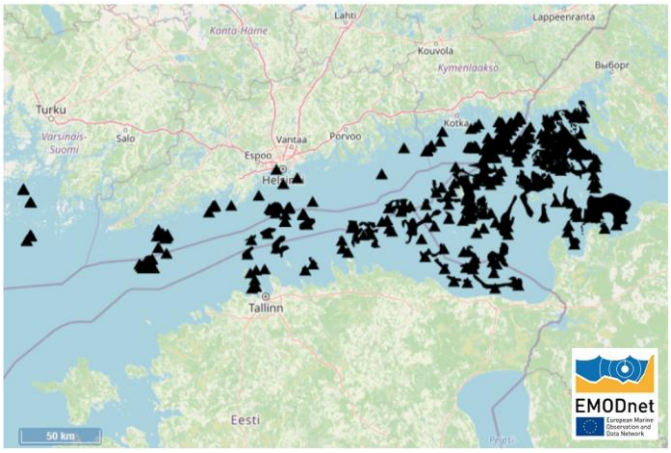

Figure 5. Spatial distribution of Fe–Mn concretion occurrences in the Gulf of Finland (EMODnet Geology Portal, accessed 15 July 2025).

Although concretions in the Baltic Sea were first noted in the late 19th century, systematic research began only in the 1960s and 1970s. Interest has increased in recent decades due to their role as environmental archives, microbial habitats, and potential as critical metal resources. Baltic Sea Fe–Mn concretions are typically porous and occur in several morphological forms, including spheroidal, discoidal, and crustal types (Figure 6). Their growth rates in the Gulf of Finland, typically around 0.01 to 0.03 mm yr^{-1}, are considerably higher than those of deep-ocean nodules, which generally grow at rates of only a few millimetres per million years (Wasiljeff et al., 2024; Shulga et al., 2025).

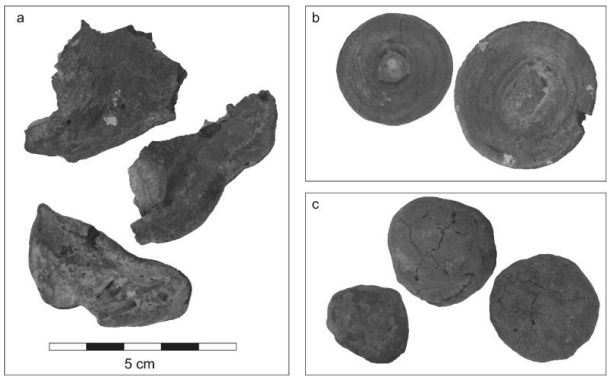

Figure 6. Morphological types of Baltic Sea Fe–Mn concretions: (a) crustal, (b) discoidal, and (c) spheroidal (Wasiljeff et al., 2024).

Fe–Mn concretions generally form in well-oxygenated seafloor environments characterised by low sedimentation rates and limited organic matter input. Periodic deposition of organic-rich, unconsolidated mud can create short-lived suboxic conditions. Alternating redox conditions control

the dissolution and reprecipitation of Fe and Mn oxyhydroxides (Wasiljeff et al., 2025b). In addition to iron, manganese, and phosphorus, concretions may contain trace elements, such as cobalt, nickel, vanadium, zinc, and rare earth elements (Majamäki et al., 2025).

In the Baltic Sea, Fe–Mn concretion formation is controlled by hydrodynamic conditions, redox processes, and the input of terrigenous material derived from land (Figure 7d). In higher-energy environments with stronger bottom currents, iron-rich crustal concretions typically form (Figure 7a–b). These areas are periodically covered by organic-rich mud, which lowers oxygen levels in surface sediments and promotes the dissolution of manganese oxides, while iron reprecipitates as poorly crystalline oxyhydroxides. Repeated depositional and erosional cycles favour the growth of iron-rich layers. Low-energy environments favour the formation of manganese-rich discoidal and spheroidal concretions (Figure 7c), where manganese is remobilised from sediments and accumulates with the assistance of microbial activity. These contrasting environmental conditions produce distinct concretion morphologies (Wasiljeff et al., 2025b).

Concretion types also differ in their magnetic and mineralogical properties. Iron-rich crustal concretions exhibit strong magnetic signals due to minerals such as magnetite and goethite, whereas manganese-rich spheroidal concretions show weaker signals and contain finer-grained, partially biogenic magnetite (Wasiljeff et al., 2024).

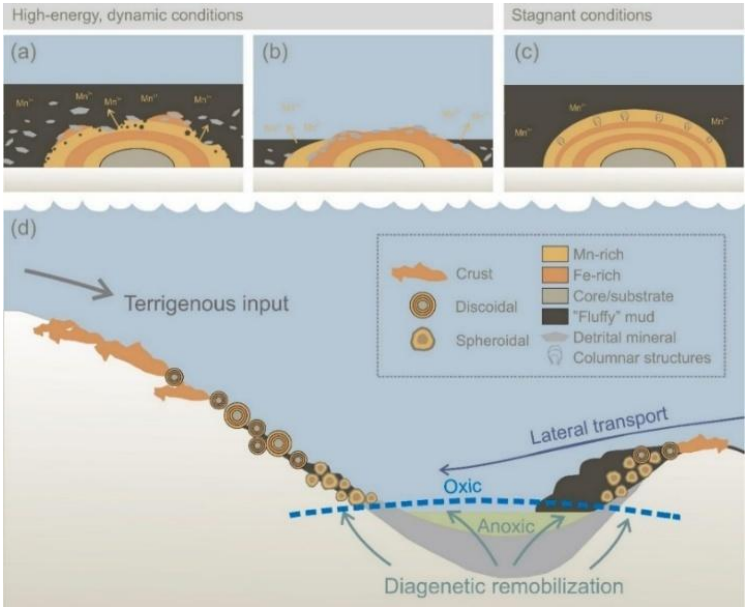

Figure 7. Formation of Fe–Mn concretions under different environmental conditions: (a-b) high-energy, oxic conditions; (c) low-energy, suboxic conditions; (d) conceptual model of environments and concretion types (Wasiljeff et al., 2025b).

Sedimentation in the Gulf of Finland is strongly influenced by riverine input, which delivers approximately one million tonnes of suspended material annually. Although some areas experience little or no sedimentation, overall rates are still higher than in deep-ocean settings where metalliferous nodules typically form. Surface concretions in the gulf generally contain higher iron and lower manganese contents than those buried within sediments (Baturin, 2009).

Fe–Mn concretions remain stable under oxic bottom-water conditions but begin to dissolve when buried under anoxic conditions. In the Gulf of Finland, strong salinity stratification limits vertical water mixing and reduces oxygen exchange between the surface and bottom waters. In anoxic environments, anaerobic bacteria dominate and often form microbial mats on the seafloor. Ongoing global climate change may further expand such anoxic zones. Concretions found at depths of approximately 27–53 m have been reported to contain elevated concentrations of heavy metals (Vallius et al., 2017). They also store phosphorus and arsenic bound to iron and manganese oxides. Under anoxic conditions, microbial reduction can release these elements into the water column, potentially increasing internal nutrient loading and contributing to eutrophication (Yli-Hemminki et al., 2016).

Microbial communities around the concretions also influence iron and manganese mineral formation and dissolution (Wasiljeff et al., 2025a). For example, bacteria of the Pseudomonadota group can oxidise iron and manganese, which promotes mineral precipitation. Experimental studies have shown that microbial activity can reduce dissolved metal concentrations in water, indicating active metal uptake and an influence on the cycling of trace elements such as cobalt and nickel (Majamäki et al., 2025).

2.2. Submarine Groundwater Discharge and Pockmarks

Most dissolved substances are transported from land to sea via rivers; however, submarine groundwater discharge (SGD) has increasingly been recognised as an important additional pathway. Unlike river discharge, SGD is typically diffuse, slow, and spatially variable, making it difficult to quantify and characterise (Szymczycha & Pempkowiak, 2016). In addition to influencing nutrient and chemical fluxes, groundwater seepage may contribute to mineral formation at the seafloor, including Fe–Mn concretions. Groundwater entering the seabed can contain dissolved iron and manganese, and this input has been suggested as a potential factor controlling concretion occurrence in the Gulf of Finland. However, the specific geochemical mechanisms and the relative importance of groundwater compared to other sources remain uncertain (Voronov & Viventsova, 2004).

Submarine groundwater discharge occurs both in coastal zones and offshore. In heterogeneous aquifers, groundwater flow may become focused, leading to the formation of pockmarks, which are shallow depressions in the seafloor. These features create localised physical and geochemical gradients that differ from the surrounding sediments and often host distinct biogeochemical conditions and microbial communities (Purkamo et al., 2022).

Pockmarks are depressions found on the floors of oceans, seas, and lakes. They form when fluids, most commonly methane-rich gas, migrate upward from subsurface sediments and accumulate beneath low-permeability layers. As fluid pressure increases, it can exceed the strength of the overlying sediments, causing deformation, fracturing, and eventual fluid escape. Gas escapes through focused pathways such as fractures, faults, or bubble plumes. Repeated seepage disturbs and removes sediment, forming a depression at the seafloor (Figure 8). Pockmarks vary in size from a few metres to several hundred metres in diameter (Vaknin et al., 2024).

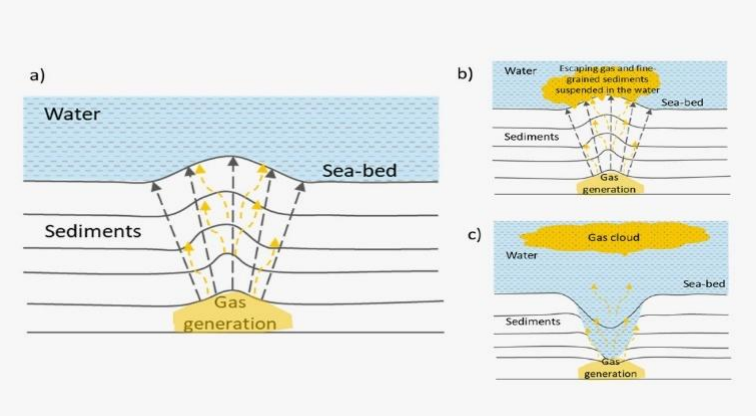

Figure 8. Conceptual model of pockmark formation: (a) gas accumulation and pressure build-up; (b) gas escape and sediment suspension; (c) development of a pockmark and continued seepage (Chopra & Marfurt, 2023).

Globally, SGD is an important mechanism for transporting nutrients and trace elements into coastal zones, where it can enhance marine biological productivity. It also introduces microorganisms from terrestrial subsurface environments into marine ecosystems. However, the interactions between groundwater-derived microbes and marine microbial communities remain poorly understood (Yanuka-Golub et al., 2024).

Studies of pockmarked sediments in the southeastern Baltic Sea show that these environments are characterised by elevated methane concentrations and microbial activity, including sulphate reduction and anaerobic methane oxidation. These processes occur where reduced, methane-rich fluids rise through sediments and encounter more oxidised conditions near the sediment–water interface, which creates sharp redox gradients. As a result, pockmarks act as biogeochemical hotspots where organic matter decomposition, methane cycling, and sulphur transformations are significantly enhanced compared to surrounding seabed areas (Kanapatskiy et al., 2021).

A similar pattern has been seen in pockmark fields in the eastern Gulf of Finland, in the Russian sector of the basin, where fluids rising from below mix with oxygen-rich seawater at the seafloor. This mixing creates strong redox gradients and promotes the mobilisation and redistribution of metals such as iron and manganese. Sediments inside pockmarks have been found to contain higher amounts of these elements, suggesting an influence of subsurface fluids and low sedimentation rates (Ivanova et al., 2011).

A variety of seafloor depressions have been identified in the eastern Gulf of Finland, including large circular craters, smaller pockmarks, and linear furrows. The largest depressions, up to 100 m wide and 4 m deep, are interpreted as kettle holes formed by the melting of buried ice blocks during the Baltic Ice Lake. These features typically occur on glacial ridges where glaciolacustrine clays have been eroded and till is exposed. Unlike pockmarks, kettle holes are not related to fluid seepage. Smaller pockmarks (typically 15–20 m in diameter) are more widespread elsewhere in the gulf and are often associated with methane release or submarine groundwater discharge. Elongated furrows and V-shaped trenches around underwater elevations have also been mapped; some are likely formed by bottom currents, whereas others may be related to gas-charged sediments (Ryabchuk et al., 2020).

Recent studies in the Gulf of Finland indicate that Fe–Mn concretions frequently co-occur with seabed pockmarks and microbial mats (Mikenberg, 2024). These features are typically found in areas with little or no modern sedimentation, where older glacial or glaciolacustrine deposits, such as varved clays or till, form the seafloor. Pockmarks associated with Fe–Mn concretion fields are commonly up to 3 m deep and 30–60 m wide and often exhibit steep to near-vertical walls. White microbial mats commonly occur inside these pockmarks, on their walls, and within adjacent concretion fields (Liira et al., 2024).

3. Study Area and Material

The four study areas are located in the Estonian waters of the Gulf of Finland, the easternmost sub-basin of the Baltic Sea (Figure 9). The investigated sites lie offshore northern Estonia, in the vicinity of Vaindloo and Mohni islands (Figure 10). Vaindloo Island is situated between study areas 1 and 2, whereas Mohni Island lies to the southwest of study area 4 (not shown in the figure). Water depths in the study areas range between approximately 30 and 90 m. The areas are located outside the main modern mud accumulation zones, and late-glacial deposits are therefore commonly exposed on the seabed.

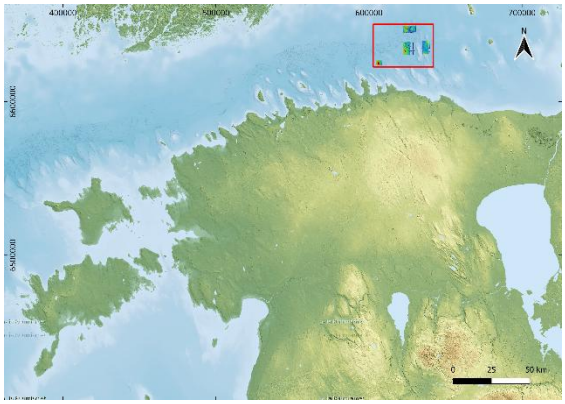

Figure 9. Location of the study areas in the Gulf of Finland (base map from the Estonian Land and Spatial Development Board, 2025a, 2025b).

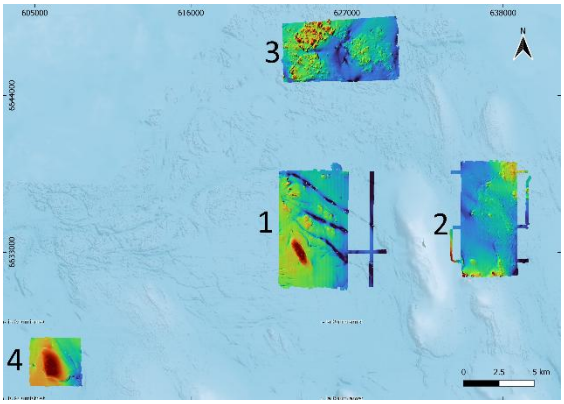

Figure 10. Detailed view of the study areas in the Gulf of Finland (base map from the Estonian Land and Spatial Development Board, 2025a, 2025b).

The study areas were selected based on previous marine geological surveys that documented Fe–Mn concretions along with associated seabed features, including pockmarks and microbial mats. These investigations were guided by earlier regional geological mapping of the Gulf of Finland conducted during Soviet-era research vessel (R/V) *Marina* expeditions at a scale of 1:200,000, which identified extensive Fe–Mn concretion-bearing areas in the region (Lutt & Raukas, 1993). The seabed geomorphology is of glacial origin and is characterised by streamlined landforms and intervening depressions, creating local variability in slope and sediment thickness, as well as sediment distribution. A more detailed description of the study areas, together with geophysical data, sediment characteristics, and visual seabed observations, is provided in the Results chapter.

This study forms part of ongoing international marine geological research in Estonian waters involving the Geological Survey of Estonia, Tallinn University of Technology, University of Tartu, Geological Survey of Finland, Norwegian Geological Survey, Stockholm University, and other partner institutions. It is connected to the Estonian Research Council project TEM-TA122 “Iron–manganese concretions of the Estonian marine area: distribution, formation mechanisms and economic potential” (2025–2028). The project focuses on the distribution, formation mechanisms, and potential economic and environmental significance of Fe–Mn concretions (Estonian Research Information System, 2025). The study is also linked to the international SECUCOAST project, which investigates groundwater–seawater interactions in coastal environments. In Estonia, this mainly involves submarine groundwater

discharge and its influence on marine environmental processes, including nutrient inputs and seabed dynamics (SecuCoast, n.d.).

The dataset used in this study consists of multibeam bathymetry, chirp sub-bottom profiler data, boomer seismic profiler data, sediment cores, Fe–Mn concretion occurrence records, and remotely operated vehicle (ROV) observations acquired during multiple marine geological and hydrographic surveys in the Gulf of Finland between 2022 and 2025.

The first survey was conducted in September 2022 aboard the R/V *Electra* (Stockholm University), during which high-resolution multibeam echosounder (MBES) and seismoacoustic data (boomer, chirp, and pinger) were collected. Sediment, porewater, and Fe–Mn concretion samples were obtained, and initial visual seabed observations were made using an underwater camera.

In April 2023, all study areas were surveyed aboard the hydrographic vessel *Jakob Prei* (Estonian State Fleet) using multibeam bathymetry and chirp sub-bottom profiling systems. Additional boomer seismic profiling, carried out by the Geological Survey of Estonia using wider survey-line spacing, improved penetration depth and subsurface stratigraphic interpretation.

In August 2023, an international marine geology expedition aboard the vessel *EVA-316* (Estonian State Fleet) was conducted to investigate the distribution and formation of Fe–Mn concretions in the Gulf of Finland. Sediment, porewater, and Fe–Mn concretion samples were collected using a GEMAX corer, a grab sampler, and an ROV equipped with manipulator arms and a push corer. The ROV, rented from the Norwegian University of Science and Technology, enabled high-resolution video documentation of pockmarks, Fe–Mn concretions, and microbial mats. An additional expedition was conducted in September 2023 aboard R/V *Salme* (Tallinn University of Technology) to collect Fe–Mn concretion and sediment samples.

In July 2025, further sampling was conducted aboard R/V *Salme* within the framework of the TEM-TA122 project. Sediment samples were collected using a GEMAX-type corer and Fe–Mn concretions using a grab sampler. In September 2025, a final expedition was conducted aboard R/V *Electra* as part of the SECUCOAST project. Fieldwork focused on marine areas in the Tallinn Bay area, around the Juminda and Ihasalu peninsulas, and near Mohni Island (study area 4). Sediment samples were collected using a box corer and a gravity coring system. ROV observations were also conducted.

Multibeam bathymetry and chirp sub-bottom profiler data used in this study were primarily acquired by the Estonian Transport Administration during hydrographic mapping of Estonian marine areas. The hillshade bathymetric visualisations used in this study were processed by Vladimir Karpin (Estonian Transport Administration). Boomer seismic profiler data and supporting geological interpretation datasets were provided by the Geological Survey of Estonia. Information on Fe–Mn concretion occurrences and historical sediment cores was compiled from Soviet-era R/V *Marina* expeditions conducted during regional geological mapping campaigns in the Gulf of Finland (Talpas et al., 1989).

The author participated in several of these expeditions and contributed to data and sample collection, including the August 2023 cruise aboard the vessel *EVA-316,* the July 2025 cruise aboard R/V *Salme*, and the September 2025 cruise aboard R/V *Electra*.

The interpreted geophysical dataset consists of chirp sub-bottom profiler and boomer seismic profiler data collected during hydrographic and marine geological surveys in the Gulf of Finland, with an average profile spacing of approximately 150 m. In total, about 645 km of chirp data and 158 km of boomer data were processed and interpreted (Table 1). This master's thesis is primarily based on the interpretation of these geophysical datasets together with supporting sedimentological and visual seabed observations. Chirp data provided denser spatial coverage and higher-resolution imaging of the shallow subsurface. Boomer profiles had wider spacing and therefore sparser coverage but offered greater penetration depth (see Appendices 1 and 2 for trackplots). Together, these datasets provide a regional framework for interpreting sediment stratigraphy, seabed geomorphology, gas-related acoustic features, and the distribution of Fe–Mn concretions within the study areas.

Table 1. Overview of interpreted seismoacoustic dataset coverage used in this study.

Data type	**Total profile length (km)**	**Coverage characteristics**
Chirp	645	Dense coverage, high-resolution shallow subsurface imaging
Boomer	158	Sparser coverage, greater penetration depth

4. Methods

The study of submarine geomorphology requires integration of multiple datasets to characterise both seafloor morphology and subsurface geological structure. Multibeam bathymetry provides high-resolution topographic data, whereas backscatter data help distinguish seabed texture and sediment type. Sub-bottom profiling images shallow subsurface stratigraphy, and sediment cores offer direct information on sediment composition and depositional history. Visual observations from remotely operated vehicles (ROV) are used to validate acoustic interpretations. The integration of these datasets within a geographic information system (GIS) environment enables comprehensive interpretation of seafloor features and processes (Micallef et al., 2018).

The data used in this thesis were collected during multiple marine expeditions in the Gulf of Finland between 2022 and 2025. These cruises provided complementary geophysical, geological, geochemical, and visual datasets for the four study areas.

This chapter presents the methods used in this study: multibeam bathymetry, sub-bottom profiles (chirp and boomer), ROV imagery, and sediment cores, as well as the data processing, analytical and GIS-based processing methods applied in this study. Data processing and analysis were carried out using Meridata, QGIS, and Microsoft Excel software. All spatial data were handled in the Estonian coordinate system L-EST97 (EPSG:3301), with vertical referencing to the Estonian Height System EH2000 (EPSG:9663). Positioning at sea relied on the ESTPOS GNSS network, providing an accuracy of approximately 1–3 cm horizontally and 1–5 cm vertically (Tuuling et al., 2021).

4.1. Multibeam Bathymetry and Backscatter

MBES provide high-resolution bathymetric data by emitting multiple acoustic beams in a fan-shaped swath beneath the vessel (Lurton & Lamarche, 2015) (Figure 11). Travel-time measurements are converted into depth values using sound-velocity profiles. This produces detailed digital terrain models (DTMs) (Micallef et al., 2018).

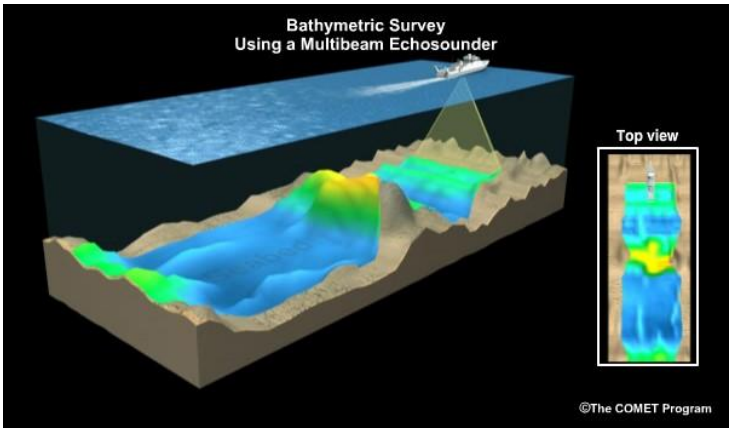

Figure 11. Multibeam bathymetric survey principle (GreenStar Technical Services JSC, n.d.).

In addition to bathymetry, MBES record backscatter intensity, which reflects seabed properties, such as sediment type, roughness, and structure (Lurton & Lamarche, 2015). Hard or coarse substrates (e.g., rock, gravel) typically produce stronger backscatter signals, whereas soft sediments (e.g., mud) produce weaker returns (Menandro et al., 2025). When properly calibrated and processed, backscatter data can be used as a quantitative indicator of seabed properties. Ground-truth data are required for reliable interpretation (Lurton & Lamarche, 2015).

Bathymetric and backscatter data used in this study were acquired by the Estonian Transport Administration during hydrographic mapping surveys using a 400 kHz multibeam echosounder. Data acquisition was carried out using a 130° swath width and a 256-beam equiangular acquisition mode. The bathymetric datasets used in this study were processed by Vladimir Karpin at the Estonian Transport Administration.

4.2. Sub-Bottom Profiling

Sub-bottom profiling uses high-frequency acoustic signals to image shallow sedimentary layers beneath the seafloor (Figure 12). These methods provide high vertical resolution but limited penetration depth, depending on frequency, source power, and sediment type (Micallef et al., 2018).

Chirp systems operate within a frequency range of 2–8 kHz and produce high-resolution images of shallow subsurface sediment layers. Boomer systems, which generate lower-frequency seismoacoustic pulses (0.5–2 kHz), can achieve greater penetration depth while maintaining good vertical resolution (Micallef et al., 2018). Together, these systems enable the identification of sediment layering, stratigraphic boundaries, deformation structures, and gas-related features (Nasif, 2024).

The chirp system used in this study achieved an average vertical resolution of approximately 0.1 m, whereas the boomer system achieved a resolution of approximately 0.4 m.

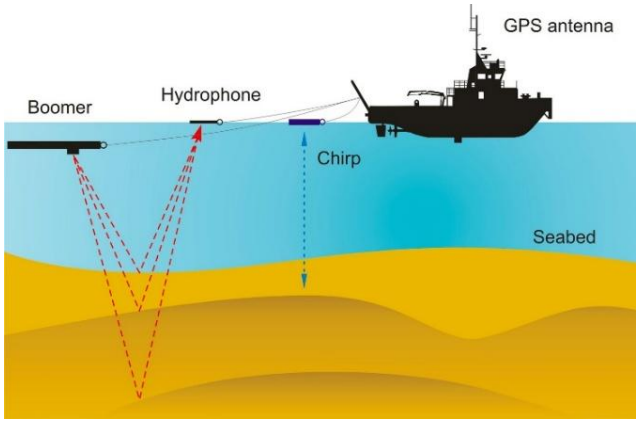

Figure 12. Sub-bottom profiling systems: boomer and chirp (adapted from Hydro International, n.d.).

4.3. Sediment Sampling

Sediment sampling methods include grab samplers and corers. Grab samplers, such as the device shown in Figure 13, collect surface sediments and Fe–Mn concretions, whereas corers recover more intact and stratified sediment sequences (Tuit & Wait, 2020).

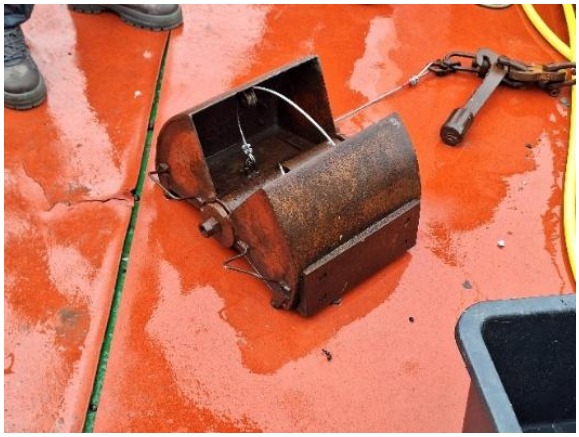

Figure 13. Grab sampler used for surface sediment and Fe–Mn concretion sampling (personal archive).

Short gravity corers (e.g., GEMAX) allow retrieval of relatively undisturbed surface sediments up to ~60 cm in length (Heinsalu et al., 2021). For deeper sampling, piston and gravity corers are used to obtain long, continuous sediment cores while minimising disturbance and compression (Figure 14). These cores offer detailed information on sediment stratigraphy and depositional history (Tuit & Wait, 2020).

Figure 14. Deployment of a gravity coring system aboard the R/V *Electra* (personal archive).

4.4. Remotely Operated Vehicles

ROVs are tethered underwater robots (Christ & Wernli, 2014) used for visual observations and targeted sampling (Figure 15). Equipped with cameras and manipulator arms, ROVs enable the direct inspection of seabed features and collection of push-core samples (Wheeler, n.d.). ROV observations are particularly valuable for validating acoustic interpretations and documenting features such as pockmarks, Fe–Mn concretions, and microbial mats.

Figure 15. AKVA Group Sub-Fighter 100K ROV aboard vessel *EVA-316* during the summer 2023 Gulf of Finland expedition (personal archive).

4.5. Data Processing

The author processed and interpreted seismoacoustic datasets using Meridata (MDPS/Profiler, release 2024.12.20) and QGIS. Bathymetric DTMs, provided by the Estonian Transport Administration and processed by Vladimir Karpin, were visualised as hillshade maps (illumination: 45°, azimuth: 315°, Z-factor: 4) in QGIS to enhance seabed features. These were combined with colour-coded bathymetric models to improve interpretation. All spatial data were handled in the Estonian Coordinate System of 1997 (L-EST97; EPSG:3301) and referenced vertically to the Estonian Height System EH2000 (EPSG:9663). The only exception was ROV datasets collected during the *EVA-316* expedition that were originally acquired in UTM Zone 34N and subsequently transformed into the L-EST97 coordinate system.

Backscatter data were analysed alongside bathymetry to distinguish sediment types. Sub-bottom profiles (chirp and boomer; pinger data were not used) were interpreted to identify seismoacoustic units (SUs), reflectors, erosion surfaces, and zones of acoustic disturbance potentially related to gas or fluid flow. All available profiles were examined and interpreted. Three-dimensional visualisation in Meridata improved the spatial understanding of the relationships between subsurface structures and seabed geomorphology.

Basic signal processing was applied to seismic data, including band-pass filtering and trace stacking. Automatic gain control was avoided to preserve relative amplitude variations. For the chirp data, a band-pass filter of 1.5–8 kHz was applied, and for the boomer data, a band-pass filter of 0.5–3 kHz. For the boomer data, envelope processing was applied to improve reflector continuity and reduce interference from the full-wave signal. Depth conversion from two-way travel time was performed using representative acoustic velocities: 1450 m s^{-1} for water, 1500–1550 m s^{-1} for mud and clay, 1750–1850 m s^{-1} for till, and 3500 m s^{-1} for bedrock (Flodén, 1981, 2009; Suuroja et al., 2010). These values are approximate and therefore introduce uncertainty into sediment-thickness estimates. ROV video data were analysed to document seabed conditions and validate interpretations (Johanna Maria Ojap, University of Tartu, pers. comm., 2026). Observations of Fe–Mn concretions, microbial mats, and sediment types were recorded.

Sediment core data, including gravity cores collected during the 2025 expedition and interpreted by marine geologist Sten Suuroja, were used to verify the seismoacoustic interpretations. Historical sediment and Fe–Mn concretion occurrence data from Soviet-era R/V *Marina* expeditions (Talpas et al., 1989) were also used to support the interpretation of the seismic units. The cores were collected during systematic geological mapping of the Estonian marine area carried out on a grid-based survey network in the Gulf of Finland. Sediment samples were recovered using approximately 12 m long coring tubes, and the mapping was conducted mainly at a scale of 1:200,000. Navigation during these surveys relied on radio navigation and Decca radar systems, with an estimated positional accuracy of approximately ±300 m. Therefore, these older datasets should be regarded as indicative rather than spatially precise.

The author compiled and mapped known occurrence sites of Fe–Mn concretions from multiple expeditions in QGIS. Although the spatial distribution of observations is uneven and some datasets contain positional uncertainty, the compiled dataset provides a useful overview of Fe–Mn concretion distribution patterns within the study areas.

5. Results

5.1. Seafloor Geomorphology

The study areas are located in the Gulf of Finland (Figures 9 and 10), where the seabed is strongly influenced by glacial processes. Water depths range between approximately 30 and 90 m below sea level (m b.s.l.). The regional seabed geomorphology is clearly streamlined, with elongated landforms trending northwest–southeast (NW–SE). Many of these features resemble mega-scale drumlins and can reach lengths of up to 10 km. In addition, smaller drumlins and fields of mega-scale glacial lineations are present. The consistent orientation of these landforms reflects the direction of ice flow during the last Weichselian glaciation and is also visible in the alignment of nearby peninsulas and islands. To the north of the study areas, the seabed geomorphology becomes irregular and rougher, indicating a transition towards areas where the crystalline basement of the Fennoscandian Shield approaches or reaches the seabed. Despite the consistent regional glacial morphology, the study areas differ in seabed relief, sediment distribution, and the occurrence of pockmarks and Fe–Mn concretions.

5.1.1. Seafloor Geomorphology: Study Area 1 – Vaindloo West

Study area 1 is located west of Vaindloo Island. Water depths range from approximately 59 to 82 m b.s.l. (Figure 16). The seabed is dominated by a prominent NW–SE trending ridge, over 2 km long and around 600 m wide, which forms a distinct topographic high resembling a mega-scale drumlin. Numerous circular to oval depressions are present on the ridge and are interpreted as pockmarks. Their diameters range from approximately 15 to 150 m, and depths reach up to approximately 4 m. In the eastern part of the ridge, some pockmarks display slightly raised rims. Fe–Mn concretion occurrence sites are concentrated along the ridge.

Additional isolated pockmarks occur outside the main ridge, particularly towards the north. In the northwestern part of the study area, smaller pockmarks are associated with a group of low, mound-like features that also coincide with Fe–Mn concretion occurrences. Several elongated depressions are also visible across the study area. Three prominent trench-like features trend NW–SE. Shallow linear depressions are also locally visible along the flanks of the main ridge and along the northern flanks of some of the smaller mound-like features. Additional shallower depressions oriented approximately west–east occur in the southwestern part of the area.

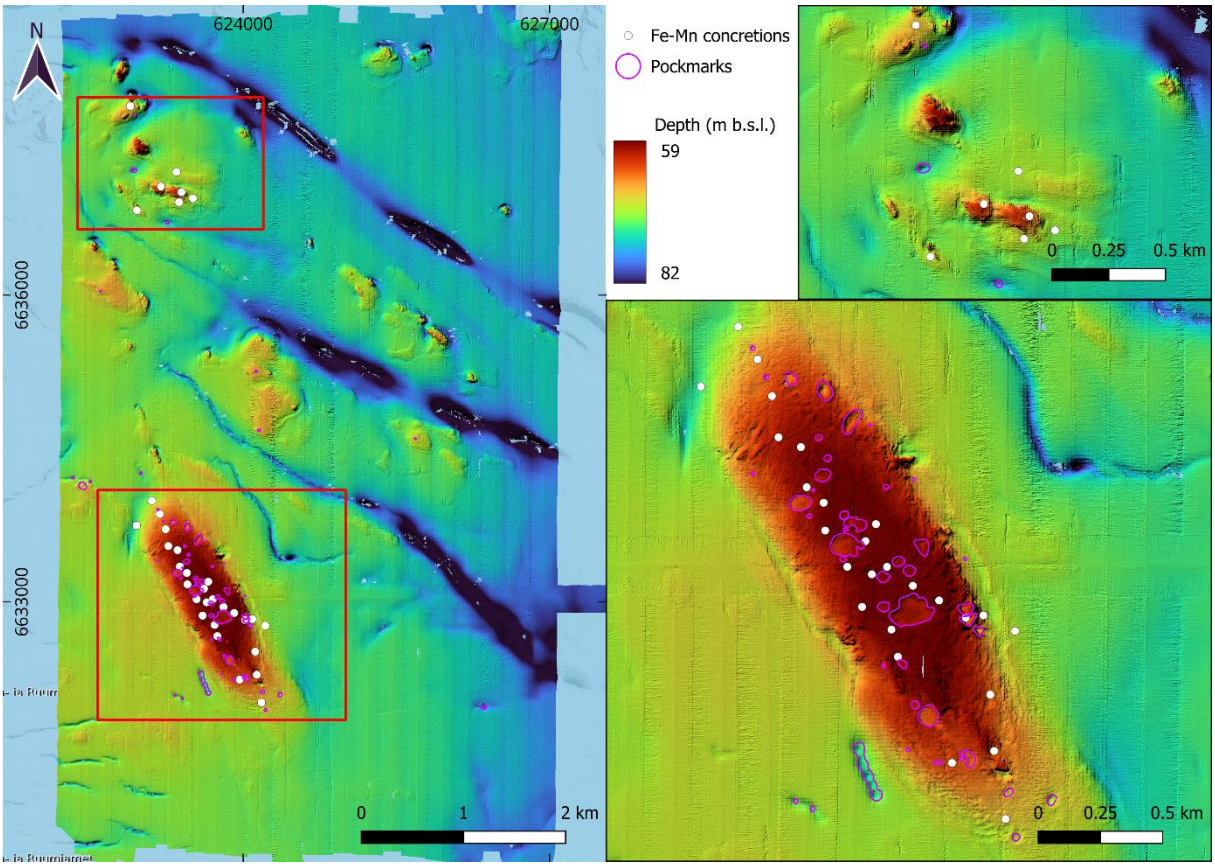

Figure 16. Digital terrain model of study area 1. Colours indicate water depth (m b.s.l.). Purple outlines show mapped pockmarks, and white dots mark Fe–Mn concretion occurrence sites from the R/V *Marina* expeditions (1980s) and the R/V *Salme* survey (2025). Insets show detailed views of the main ridge and adjacent northern mound features.

5.1.2. Seafloor Geomorphology: Study Area 2 – Vaindloo East

Study area 2 is located east of Vaindloo Island. Water depths range from approximately 34 to 76 m b.s.l. (Figure 17). The seabed is characterised by elongated NW–SE trending landforms consistent with the regional glacial pattern. Compared to study area 1, the overall relief is smoother and less pronounced. In the northern and central parts of the area, several small mound-like landforms are associated with shallow erosional depressions on their northern flanks. Towards the south, the seabed becomes slightly rougher, with more pronounced relief and several elevated mounds. In the southeastern part, a group of smaller moraine ridge-like features is present.

A zoomed view of the central area reveals a rough erosional terrain characterised by numerous small ridges, shallow depressions, and irregular linear features. Within this zone, several circular depressions interpreted as pockmarks are observed. These features are relatively small, typically 30–40 m in diameter and approximately 1 m deep. Fe–Mn concretions are concentrated within this rough terrain, and their distribution follows the same NW–SE orientation as the surrounding landforms.

Although the overall relief in study area 2 is less pronounced than in other study areas, the concretion-bearing and pockmark-rich terrain is still surrounded by relatively deeper and smoother seabed areas that represent local sediment accumulation zones.

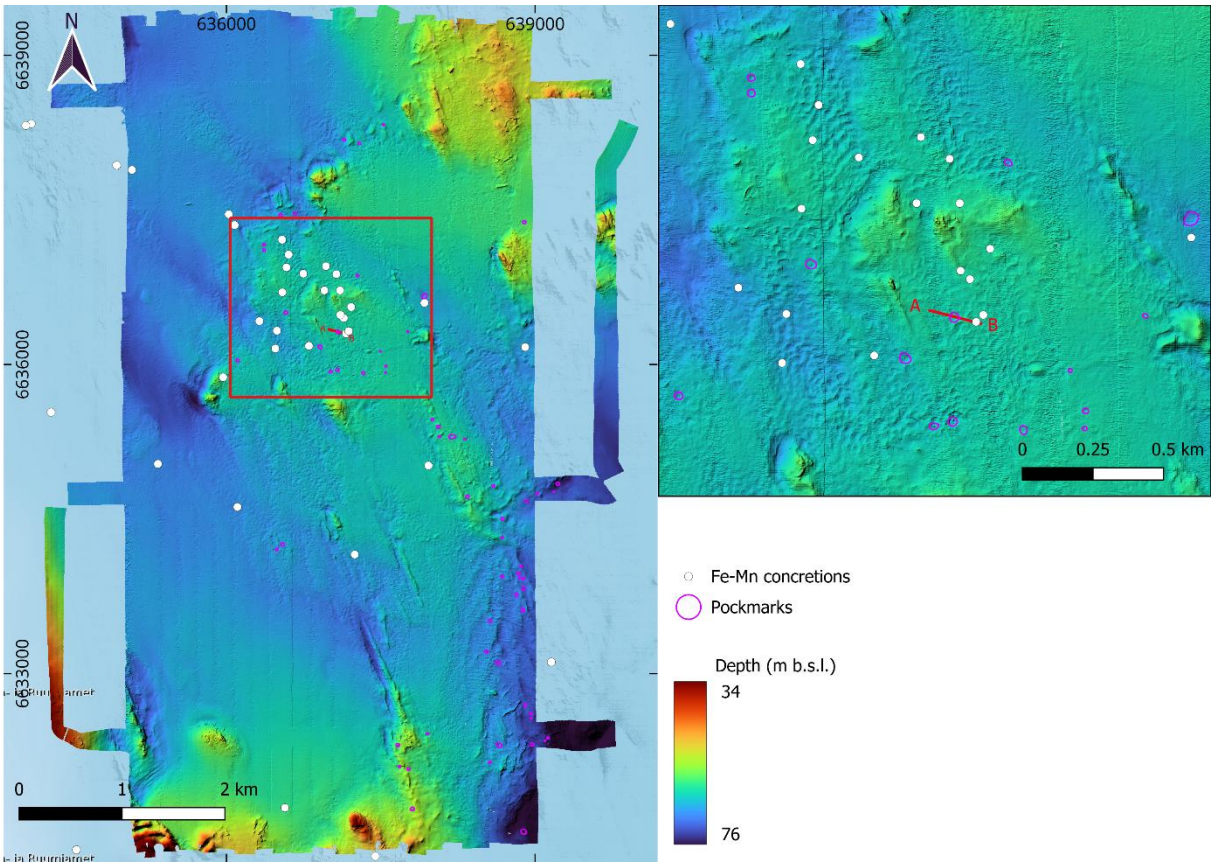

Figure 17. Digital terrain model of study area 2. Colours indicate water depth (m b.s.l.). Purple outlines show mapped pockmarks, and white dots mark Fe–Mn concretion occurrence sites from the R/V *Marina* expeditions (1980s) and the R/V *Salme* survey (2025). The inset shows a detailed view of the erosional terrain, where a short A–B transect across a pockmark is indicated for bathymetric profiling (see Figure 18).

A representative pockmark is shown in Figure 18 together with a bathymetric profile. The pockmark is circular and approximately 35 m in diameter. The profile clearly shows a well-defined depression with a distinct central high, which is a recurring feature in several pockmarks within the area. Outside the pockmark, the bathymetric profile also shows irregular small-scale seabed relief consistent with the surrounding erosional terrain.

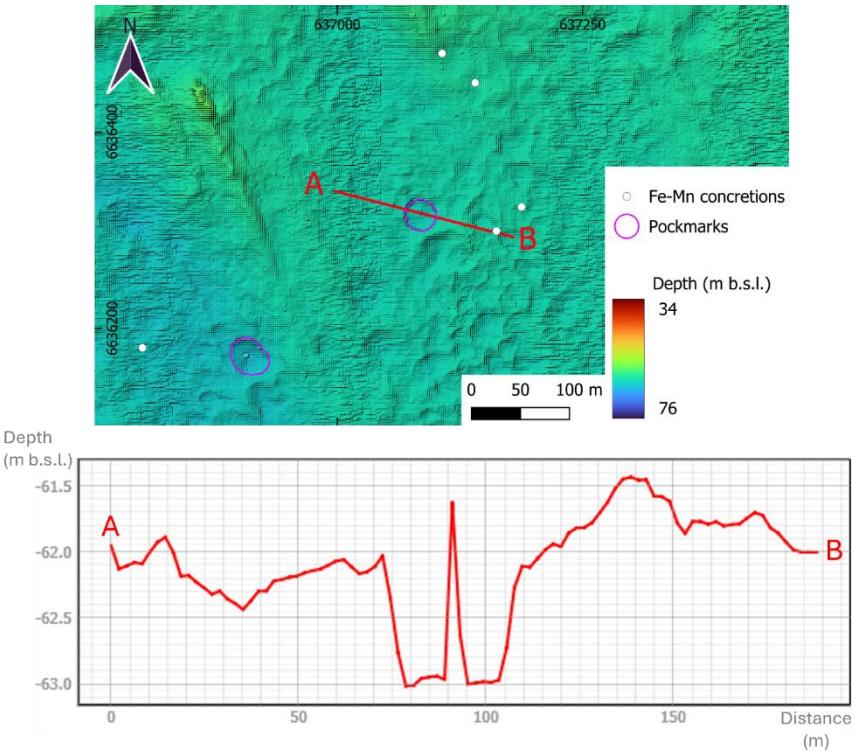

Figure 18. Representative pockmark and corresponding bathymetric profile in study area 2. Purple outlines show mapped pockmarks, and white dots mark Fe–Mn concretion occurrence sites from the R/V *Marina* expeditions (1980s) and the R/V *Salme* survey (2025).

5.1.3. Seafloor Geomorphology: Study Area 3 – Vaindloo North

Study area 3 is located north of Vaindloo Island. Water depths range from approximately 37 to 81 m b.s.l. (Figure 19). The seabed geomorphology is more irregular than in the previous study areas. The area is characterised by clusters of elevated, mound-like landforms forming zones of rugged relief. Three main clusters can be distinguished: two in the western part and one in the eastern part. These are separated by a deeper and smoother central basin. The northwestern cluster is the shallowest and most irregular, lacking a clear streamlined morphology. The southwestern and eastern clusters contain more elongated NW–SE trending landforms resembling smaller drumlins.

Pockmarks and Fe–Mn concretion occurrences are mainly associated with these elevated areas. Pockmarks are generally circular to oval and relatively small, typically around 20 m in diameter, although some reach up to approximately 100 m. The depth of the pockmarks can reach up to approximately 3 m. Many of the smaller pockmarks exhibit a central elevation similar to those observed in study area 2. The deep central basin lacks both pockmarks and recorded Fe–Mn concretion occurrences.

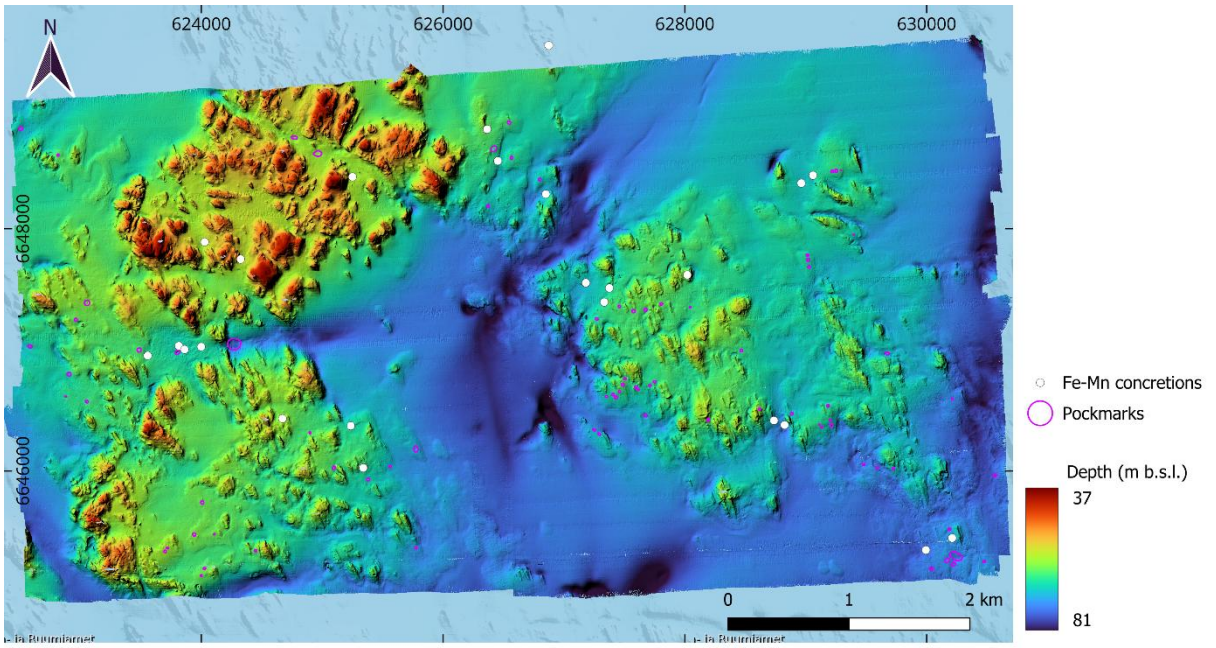

Figure 19. Digital terrain model of study area 3. Colours indicate water depth (m b.s.l.). Purple outlines show mapped pockmarks, and white dots mark Fe–Mn concretion occurrence sites from the R/V *Marina* expeditions (1980s) and the R/V *Salme* survey (2025).

5.1.4. Seafloor Geomorphology: Study Area 4 – Mohni

Study area 4 is located northeast of Mohni Island and is the smallest of the study areas. Water depths range from approximately 65 to 90 m b.s.l. (Figure 20). The seabed is dominated by a single prominent ridge-like feature that forms a distinct topographic high approximately 2.5 km long and up to 1.5 km wide. This structure resembles the drumlin-like ridge observed in study area 1. The surrounding seabed is deeper and relatively flat, with several shallow linear depressions locally visible along the flanks of the main ridge.

Numerous pockmarks are present on the surface of the ridge. These pockmarks vary in size, with larger ones reaching diameters of approximately 100–200 m and smaller ones ranging from 10 to 40 m. Pockmark depths reach up to 4 m. The smaller pockmarks often have steeper and more sharply defined edges, whereas larger ones tend to be broader with gentler slopes. Fe–Mn concretions are concentrated on the ridge and spatially associated with pockmarks. The surrounding flat seabed shows no clear evidence of pockmarks or concretion occurrences.

A representative large pockmark is shown in Figure 21 with a bathymetric profile. The feature has a diameter of approximately 180 m and is characterised by a broad, smooth depression. A subtle central elevation is present, although it is less pronounced than in smaller pockmarks observed in other study areas.

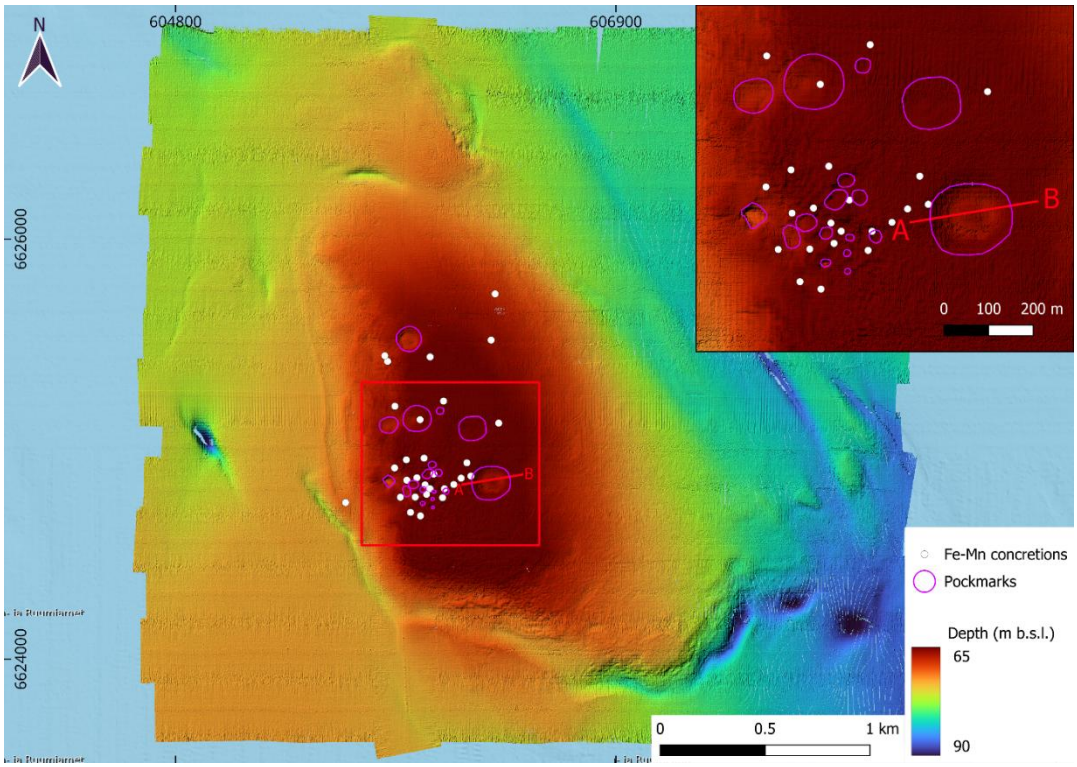

Figure 20. Digital terrain model of study area 4. Colours indicate water depth (m b.s.l.). Purple outlines show mapped pockmarks, and white dots mark Fe–Mn concretion occurrence sites from the R/V *Marina* (1980s) and the R/V *Salme* surveys (2023 and 2025). The inset shows a detailed view of clustered smaller pockmarks on the ridge, where a short A–B transect across a pockmark is indicated for bathymetric profiling (see Figure 21).

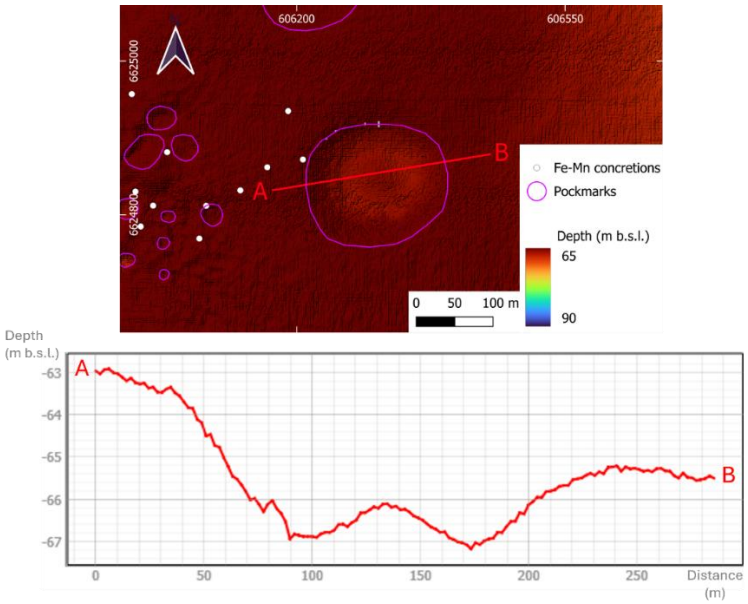

Figure 21. Representative pockmark and corresponding bathymetric profile in study area 4. Purple outlines show mapped pockmarks, and white dots mark Fe–Mn concretion occurrence sites from the R/V *Marina* expeditions (1980s) and the R/V *Salme* surveys (2023 and 2025).

5.2. Seismostratigraphy

In this study, seismostratigraphy refers to the interpretation of acoustically distinguishable sedimentary units identified from chirp sub-bottom and boomer seismic profiles. Because the interpretation is based primarily on acoustic characteristics rather than direct lithological observations, the units are termed seismoacoustic units (SU1–SU7). Representative profiles were selected for each study area to illustrate the general seismoacoustic structure and its relationship to seabed geomorphology. Gas-related acoustic disturbances identified in the seismic profiles are referred to as "GAS". These features are interpreted as zones where shallow gas accumulations within organic-rich upper sediments attenuate or obscure deeper acoustic reflections. The mapped "GAS" zones therefore represent areas of acoustic masking rather than gas occurrence throughout the entire sedimentary succession.

Representative profiles were selected for each study area to illustrate the general seismoacoustic structure and its relationship to seabed geomorphology. Although chirp data provide significantly wider coverage than boomer data (Appendices 1 and 2), both chirp and boomer profiles were interpreted. The chirp dataset was designed to provide dense spatial coverage across the study areas, whereas the more widely spaced and sparse boomer profiles were used to image deeper subsurface structures. Where available, additional profiles intersecting sediment core locations were used to compare seismic interpretation with lithological data. Figure 22 presents a schematic stratigraphic succession of the Gulf of Finland based on geological literature and illustrates the relationship between regional geology and the interpreted seismoacoustic units. It summarises the main lithological units and their depositional environments, and their potential correspondence to the interpreted seismoacoustic units (SU1–SU7).

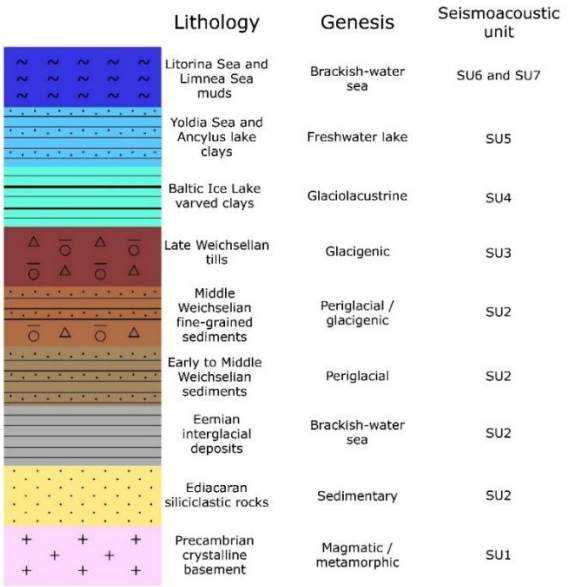

Figure 22. Idealised stratigraphic succession of the Gulf of Finland showing major lithological units, depositional environments, and their interpreted correspondence to seismoacoustic units SU1–SU7 (compiled by the author based on published literature).

Based on the regional geological framework, the interpreted seismoacoustic units can be tentatively correlated with known geological units of the Gulf of Finland. SU1 is interpreted as crystalline basement forming a continuous high-amplitude reflector. SU2 likely represents older sedimentary or periglacial and/or glacigenic deposits of uncertain origin. SU3 is interpreted as Late Weichselian till. SU4 corresponds to glaciolacustrine varved clay deposited during the Baltic Ice Lake stage, whereas SU5 represents Yoldia Sea and Ancylus Lake deposits. The uppermost units, SU6 and SU7, are interpreted as younger postglacial sediments of the Litorina and Limnea Sea stages. These correlations should be regarded as tentative.

5.2.1. Seismostratigraphy: Study Area 1 – Vaindloo West

Figure 23 presents a three-dimensional visualisation of the interpreted seismoacoustic units (SU1–SU7) and gas-related features in study area 1, based on chirp sub-bottom profiles. The subsurface structure closely reflects the seabed geomorphology described above, with a prominent ridge corresponding to the drumlin-like landform.

On the ridge, upper sediment units are thin or locally absent, whereas thicker sedimentary successions occur in the surrounding depressions. Consequently, older units occur close to the seabed or are locally exposed. Gas-related acoustic disturbances are widespread and appear as vertical zones of attenuated or obscured reflections. These features occur mainly in deeper areas surrounding the ridge, where thicker postglacial sediment units (SU5–SU7) are present.

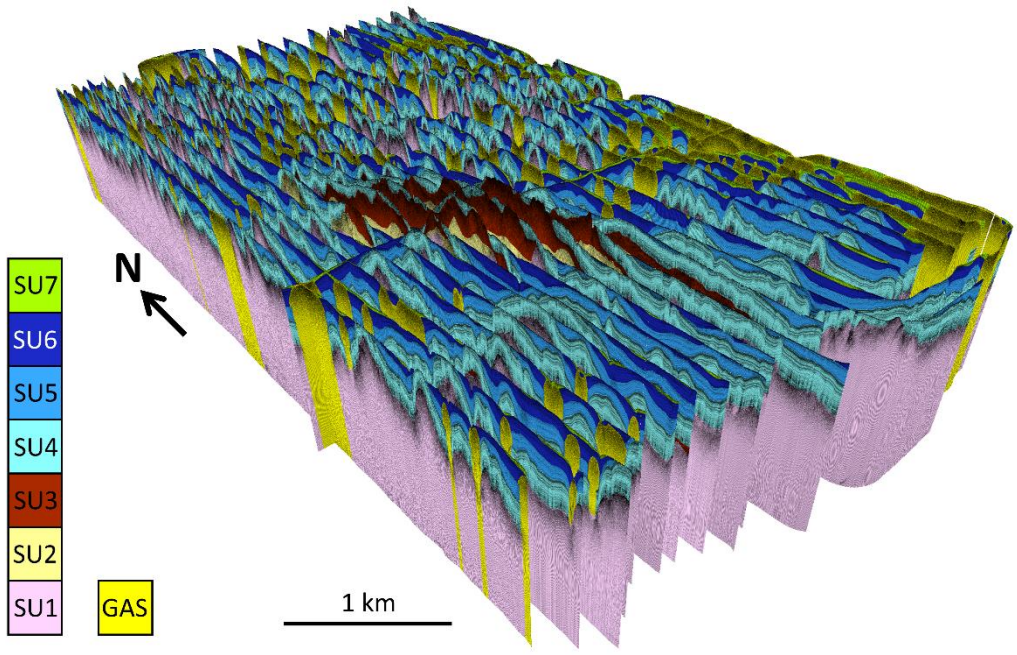

Figure 23. Three-dimensional visualisation of interpreted seismoacoustic units (SU1–SU7) and gas-related acoustic disturbances in organic-rich sediments (GAS) in study area 1 (Vaindloo West), based on chirp sub-bottom profiles.

Because the main ridge represents the most prominent geomorphological feature in this study area and contains the highest concentration of mapped pockmarks and Fe–Mn concretion occurrence sites, a representative seismic profile (Profile 1) crossing it was selected for detailed interpretation (Figure 24). Both chirp and boomer data were available along this profile line. An additional seismic profile (Profile 2), located west of the main representative profile but still crossing the same ridge structure, intersects sediment core M_87_018006 from the historical R/V *Marina* surveys.

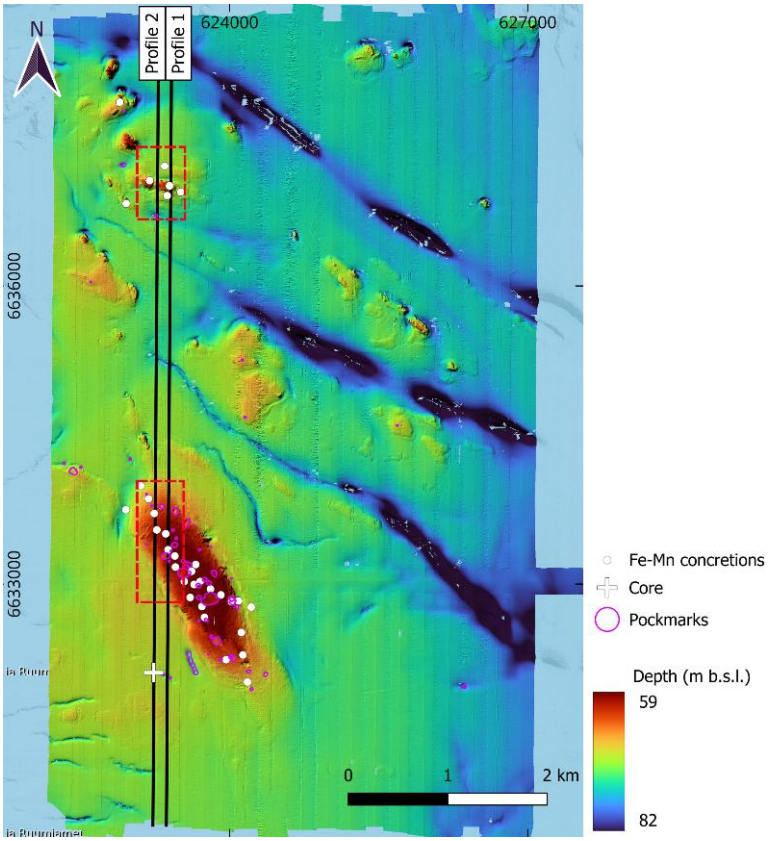

Figure 24. Location of representative seismoacoustic profiles (Profile 1 and Profile 2) and sediment core M_87_018006 in study area 1 (Vaindloo West), showing mapped pockmarks, Fe–Mn concretion occurrence sites, and inferred concretion occurrence zones (red dashed boxes).

The representative boomer profile (Figure 24, Profile 1) is shown in Figure 25. The profile reveals a layered succession composed of seven seismoacoustic units (SU1–SU7). Although the northern part of the boomer profile is locally affected by a signal-related artefact, the profile was selected because it provides the clearest overall representation of the ridge structure and deeper seismoacoustic units.

SU1 forms a continuous basal reflector interpreted as crystalline basement. Multiple reflections within this unit are considered acoustic artefacts. SU2 is restricted to the ridge area and likely represents Ediacaran siliciclastic rocks or Early to Middle Weichselian periglacial and/or glacigenic deposits. SU3 is interpreted as glacigenic sediment, most likely Late Weichselian till. It forms a relatively continuous body within the ridge area but also occurs locally as smaller discontinuous deposits elsewhere along the profile. SU4 forms one of the thickest and most continuous units and is interpreted as Baltic Ice Lake varved clay, usually reaching a thickness of approximately 10 m. SU5–SU7 represent younger

postglacial sediments, with SU7 forming only a thin uppermost layer. Gas-related disturbances are commonly associated with areas where SU7 is present. Fe–Mn concretions are mainly associated with the ridge, where older units (SU2–SU3) occur close to the seabed. Additional concretions occur in the northern part of the profile, where mound-like features coincide with exposed or shallow basement (SU1) and a thin glaciolacustrine clay layer (SU4).

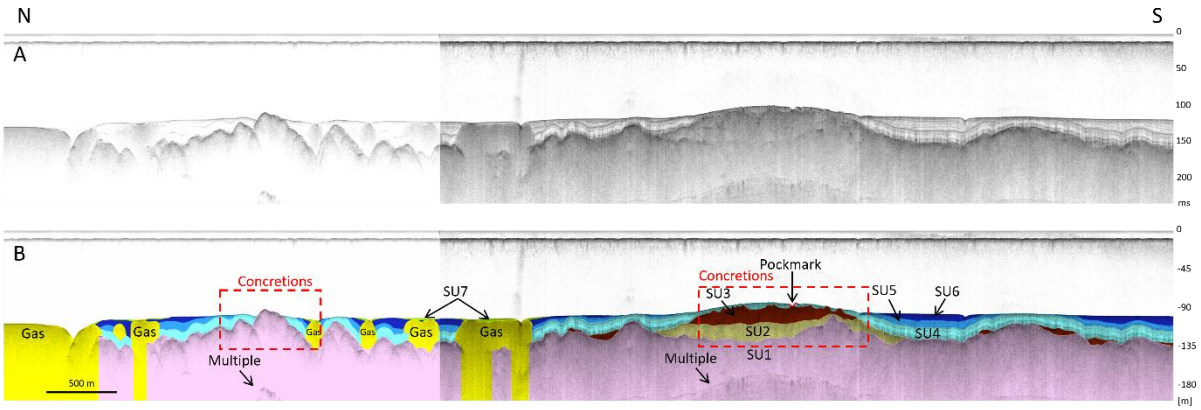

Figure 25. Boomer seismic profile across study area 1 (Vaindloo West) showing: (a) uninterpreted and (b) interpreted sections with seismoacoustic units (SU1–SU7), pockmarks, and inferred Fe–Mn concretion occurrence zones (red dashed boxes), and gas-related acoustic disturbances in organic-rich sediments (GAS).

The overall structure of the additional profile (Figure 24, Profile 2) is similar to that observed in the representative profile shown in Figure 25. The same seismoacoustic units (SU1–SU7) can be identified, with thicker and more continuous sedimentary successions in deeper basin-like areas (Figure 26). Comparison between the seismic interpretation and sediment core data shows good agreement. In particular, the boundary between SU4 and the overlying postglacial units (SU5–SU6) corresponds well with lithological changes observed in the core. Although the exact position of the core is approximate, the correlation is considered reliable because the core was recovered from a thick and laterally continuous sediment accumulation area. Overall, the stratigraphic interpretation is consistent with the lithological data.

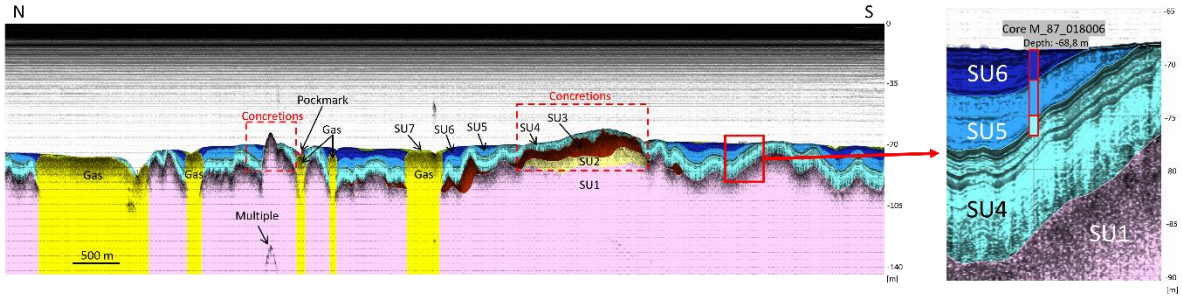

Figure 26. Chirp sub-bottom profile from study area 1 (Vaindloo West) showing interpreted seismoacoustic units (SU1–SU7), pockmarks, inferred concretion occurrence zones (red dashed boxes), and gas-related acoustic disturbances in organic-rich sediments (GAS). The inset shows sediment core M_87_018006 with corresponding stratigraphic boundaries.

5.2.2. Seismostratigraphy: Study Area 2 – Vaindloo East

Figure 27 presents a three-dimensional visualisation of the interpreted seismoacoustic units in study area 2 (Vaindloo East), based on chirp sub-bottom profiles. Compared to study area 1, the subsurface structure is simpler and laterally more uniform. The seabed is generally flat and lacks a prominent ridge-like feature. However, the southern part of the study area shows a rougher and more irregular geomorphology. No significant gas-related acoustic disturbances were identified in the interpreted profiles.

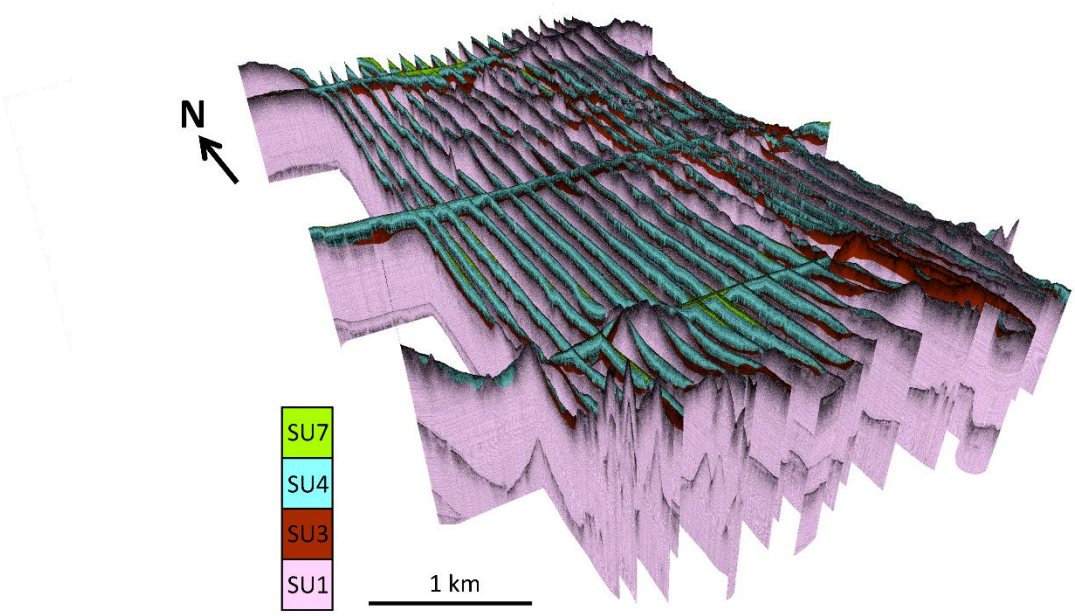

Figure 27. Three-dimensional visualisation of interpreted seismoacoustic units (SU1, SU3, SU4, SU7) in study area 2 (Vaindloo East), based on chirp sub-bottom profiles.

Two representative seismic profiles were selected for detailed interpretation (Figure 28). Profile 1 crosses the irregular geomorphological features described in the previous section and an area with numerous Fe–Mn concretion occurrence sites. Both chirp and boomer data were available along this profile line, although only the boomer profile is presented here. Profile 2, located west of Profile 1, approximately intersects historical sediment core M_86_051010 from the R/V *Marina* surveys.

The representative boomer profile (Figure 28, Profile 1) is shown in Figure 29. The profile displays a relatively simple and laterally continuous sedimentary succession dominated by SU1, SU3, and SU4. SU1 forms a continuous basal reflector interpreted as crystalline basement. Multiple reflections within SU1 and the water column in the boomer data are interpreted as acoustic artefacts. SU3 overlies the basement and varies considerably in thickness, whereas SU4 forms an upper glaciolacustrine clay layer. Unlike study area 1, no major ridge structure is present. Instead, the southern part of the profile exhibits rougher geomorphology and thicker and laterally continuous SU3 deposits. SU4 generally follows the underlying topography but locally shows clear erosional truncation, producing an uneven seabed surface consistent with the geomorphological observations. The inferred Fe–Mn concretion occurrence zone corresponds to areas where basement (SU1) and glacial deposits (SU3) occur close to the seabed beneath a thin locally eroded varved clay (SU4) layer.

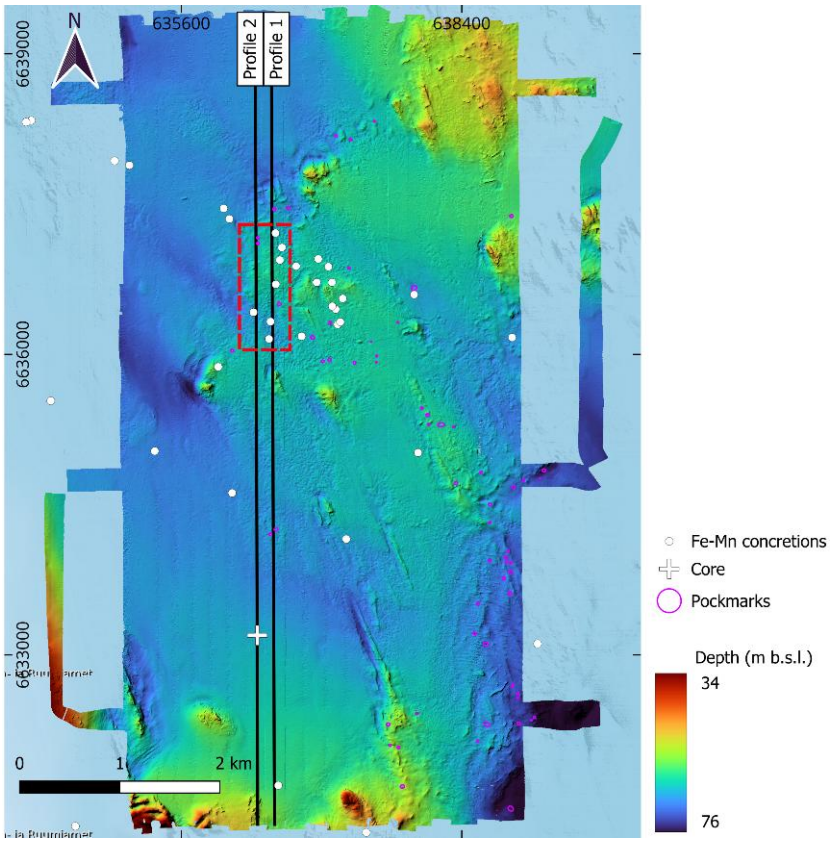

Figure 28. Location of representative seismoacoustic profiles (Profile 1 and Profile 2) and sediment core M_86_051010 in study area 2 (Vaindloo East), showing mapped pockmarks, Fe–Mn concretion occurrence sites, and the inferred concretion occurrence zone (red dashed box).

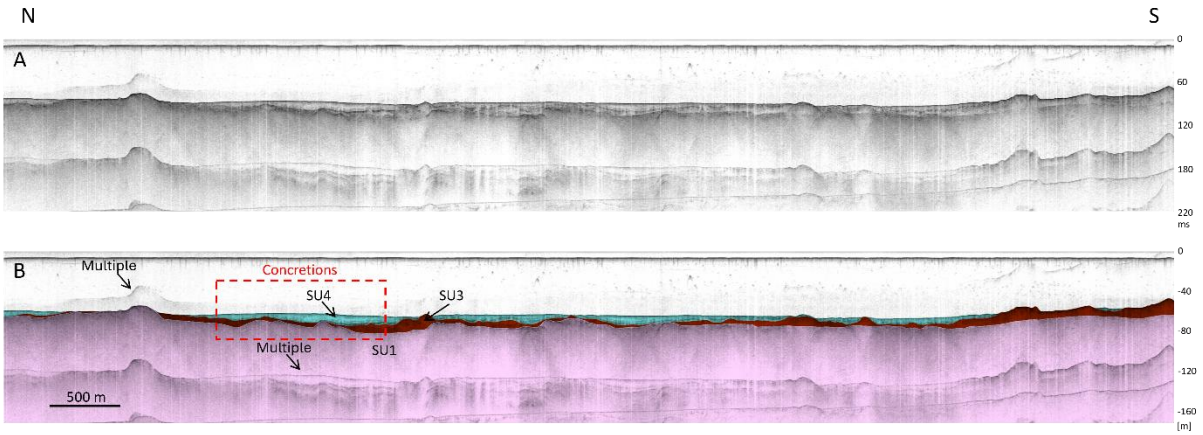

Figure 29. Boomer seismic profile across study area 2 (Vaindloo East) showing: (a) uninterpreted and (b) interpreted sections with seismoacoustic units (SU1, SU3, SU4) and the inferred Fe–Mn concretion occurrence zone (red dashed box).

Figure 30 shows the additional chirp profile (Figure 28, Profile 2). Although the overall structure resembles the representative profile, local variations are present. In the northern part of the line, the sedimentary succession is thicker and more clearly layered, whereas in the central part crystalline basement (SU1) is locally exposed or covered only by thin Late Weichselian tills (SU3). This area coincides with the inferred Fe–Mn concretion occurrence zone. The sediment core generally supports the seismic interpretation, although distinct lithological boundaries are not clearly defined. The uppermost sediments correspond well to the glaciolacustrine clay unit (SU4).

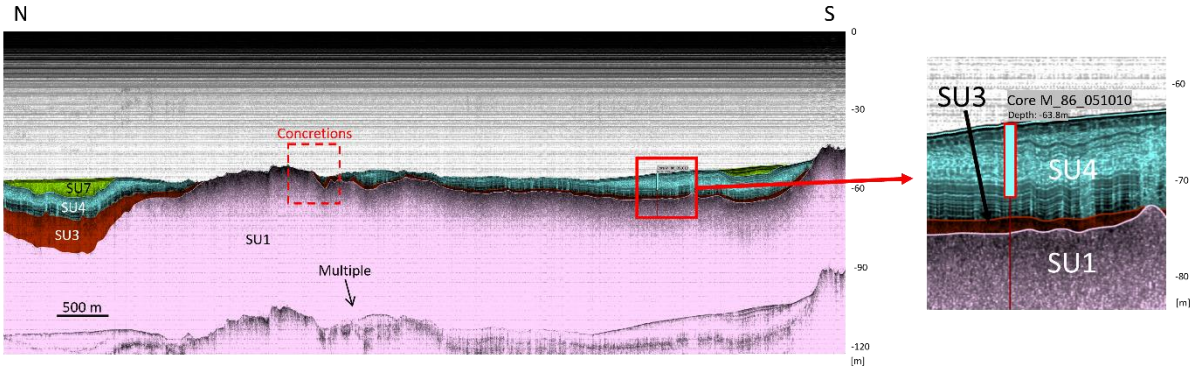

Figure 30. Chirp sub-bottom profile from study area 2 (Vaindloo East) showing interpreted seismoacoustic units (SU1, SU3, SU4, SU7) and the inferred Fe–Mn concretion occurrence zone (red dashed box). The inset shows sediment core M_86_051010 with corresponding stratigraphic boundaries.

5.2.3. Seismostratigraphy: Study Area 3 – Vaindloo North

Figure 31 presents a three-dimensional visualisation of the interpreted seismoacoustic units and gas-related features in study area 3 (Vaindloo North). Compared to the previous study areas, the subsurface structure is more complex and laterally heterogeneous.

The seabed is characterised by several elevated areas separated by deeper depressions, consistent with the rough geomorphology observed in bathymetric data. On the elevated areas, upper sediment units are commonly thin, discontinuous, or partly eroded. In these locations, crystalline basement (SU1) occurs close to the seabed or is locally exposed, while Late Weichselian tills (SU3) occur mainly as patchy deposits beneath a thin glaciolacustrine clay (SU4) layer. Younger postglacial units are largely absent from these elevated features. In the deeper areas, the sedimentary succession becomes thicker and more continuous. Units SU4–SU6 form a layered sequence, and locally, SU7 is also present. Gas-related acoustic disturbances occur mainly in these deeper sediment-filled depressions.

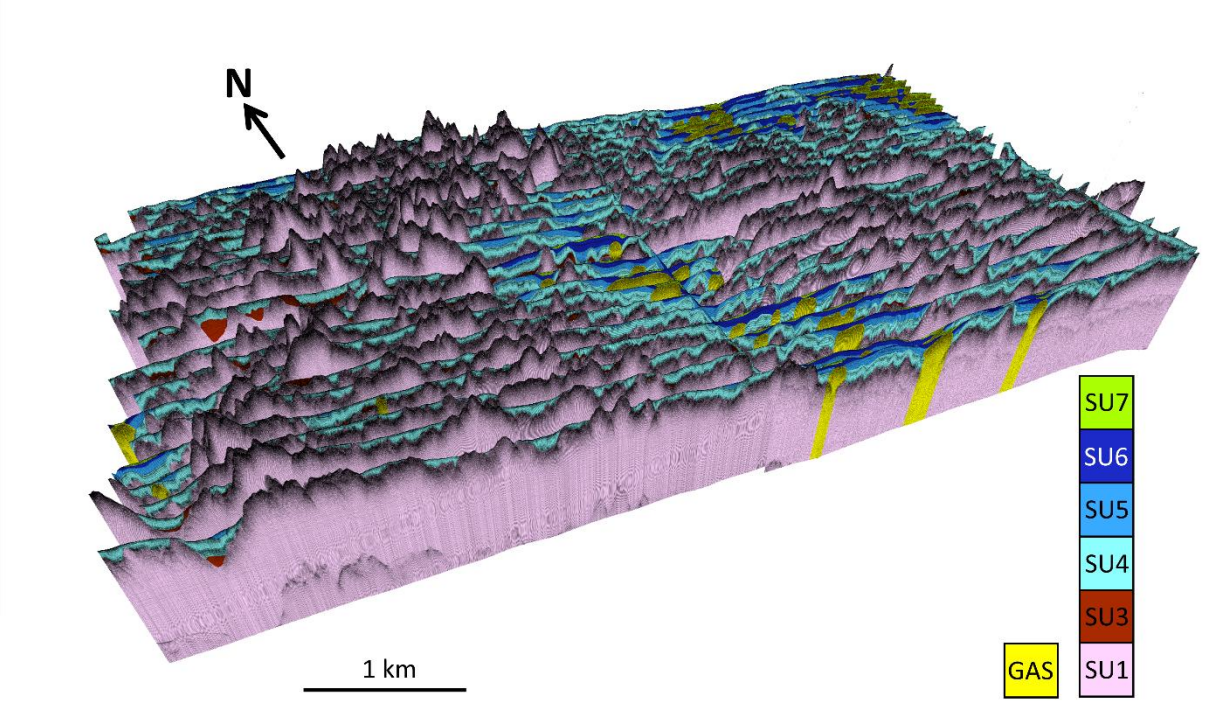

Figure 31. Three-dimensional visualisation of interpreted seismoacoustic units (SU1, SU3–SU7) and gas-related acoustic disturbances in organic-rich sediments (GAS) in study area 3 (Vaindloo North), based on chirp sub-bottom profiles.

Two representative seismic profiles were selected for detailed interpretation (Figure 32). Profile 1 crosses the main geomorphological features of the study area, including the eastern elevated area, the deeper central basin, and the area between the two western elevated areas. Pockmarks and Fe–Mn concretion occurrence sites are mainly associated with these elevated areas. Both chirp and boomer data were available along this profile line, although only the boomer profile is presented because of its greater penetration depth. Profile 2, located south of Profile 1, intersects sediment core M_87_020002 from the R/V *Marina* surveys.

The representative boomer profile (Figure 32, Profile 1) is presented in Figure 33. SU1 forms a basal reflector throughout the profile, whereas overlying units vary considerably depending on topography. Elevated areas are characterised by exposed or shallow basement, patchy SU3 deposits, and discontinuous SU4. The deeper central part of the profile contains a thicker and more complete succession composed of SU3–SU7.

Gas-related acoustic disturbances are concentrated in these deeper areas, where postglacial sediment thickness is greatest, and most likely reflects shallow gas formation related to organic matter decomposition within modern sediment accumulation zones. The inferred Fe–Mn concretion occurrence zones correspond to elevated areas where crystalline basement (SU1) occurs close to the seabed beneath a thin and eroded SU4 layer. In the western elevated area, thin glacigenic deposits (SU3) are also present between the basement and SU4.

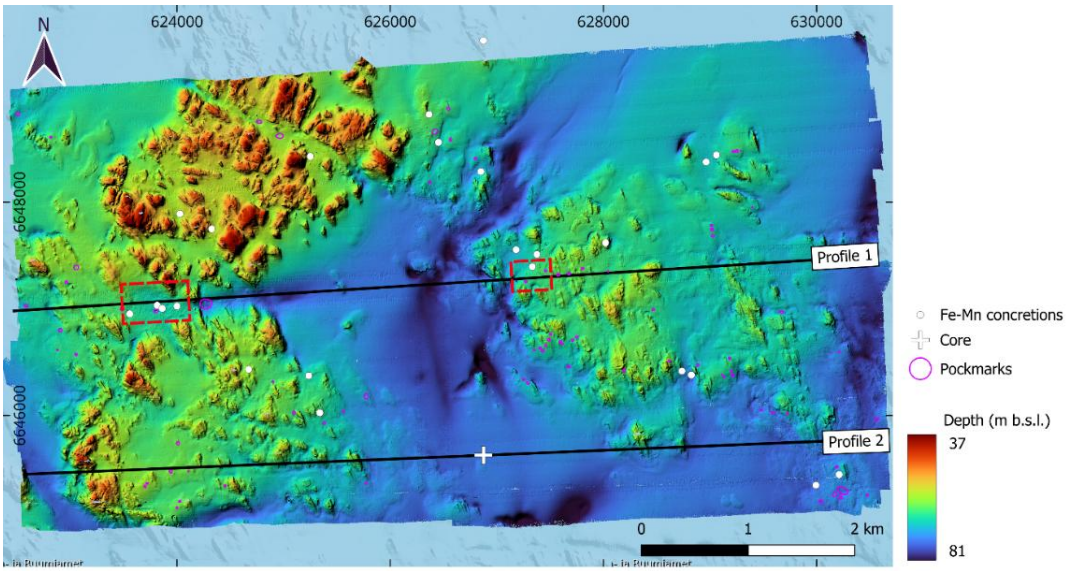

Figure 32. Location of representative seismoacoustic profiles (Profile 1 and Profile 2) and sediment core M_87_020002 in study area 3 (Vaindloo North), showing mapped pockmarks, Fe–Mn concretion occurrence sites, and inferred concretion occurrence zones (red dashed boxes).

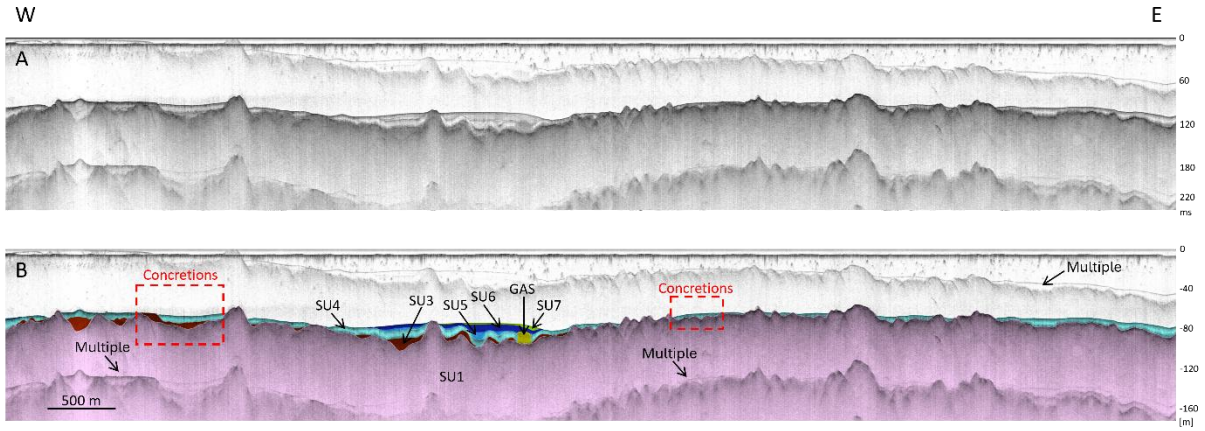

Figure 33. Boomer seismic profile across study area 3 (Vaindloo North) showing: (a) uninterpreted and (b) interpreted sections with seismoacoustic units (SU1, SU3–SU7), inferred Fe–Mn concretion occurrence zones (red dashed boxes), and gas-related acoustic disturbances in organic-rich sediments (GAS).

The additional profile (Figure 32, Profile 2) shows a generally similar stratigraphic structure to the representative profile, although the eastern elevated zone is less pronounced (Figure 34). The crystalline basement (SU1) forms the continuous basal reflector. On the elevated areas, the varved clay layer (SU4) is present but appears eroded and discontinuous. Deeper parts of the profile contain a thicker sedimentary succession of glaciolacustrine and postglacial sediments (SU4–SU7). Gas-related acoustic disturbances are again associated with thicker sediment accumulations. No Fe–Mn concretion occurrences have been identified along this profile. The sediment core supports the interpretation of a thicker sedimentary succession in deeper parts of the study area, particularly the presence of glaciolacustrine and postglacial units (SU4–SU6).

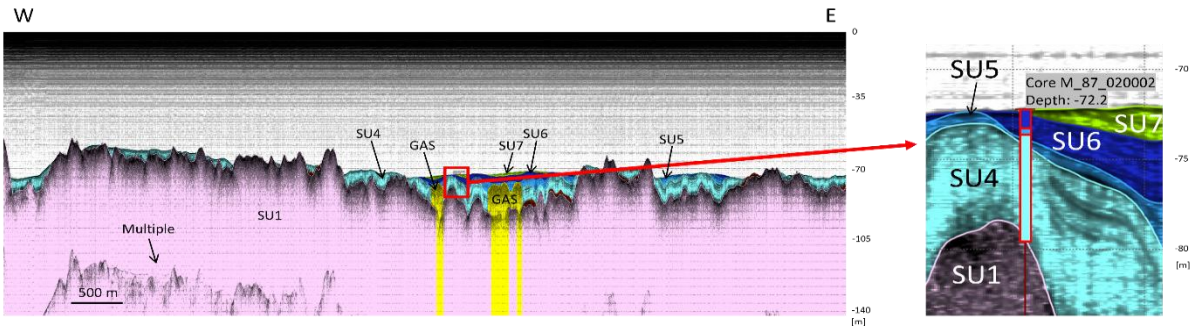

Figure 34. Chirp sub-bottom profile from study area 3 (Vaindloo North) showing interpreted seismoacoustic units (SU1, SU3–SU7) and gas-related acoustic disturbances in organic-rich sediments (GAS). The inset shows sediment core M_87_020002 with corresponding stratigraphic boundaries.

5.2.4. Seismostratigraphy: Study Area 4 – Mohni

Figures 35 and 36 present three-dimensional visualisations of the interpreted seismoacoustic units for study area 4 (Mohni), based on chirp and boomer data. Clear differences exist between the datasets: chirp profiles resolve only SU1 and the upper units (SU4–SU7), whereas the boomer data image additional intermediate units (SU2–SU3) because of greater penetration depth.

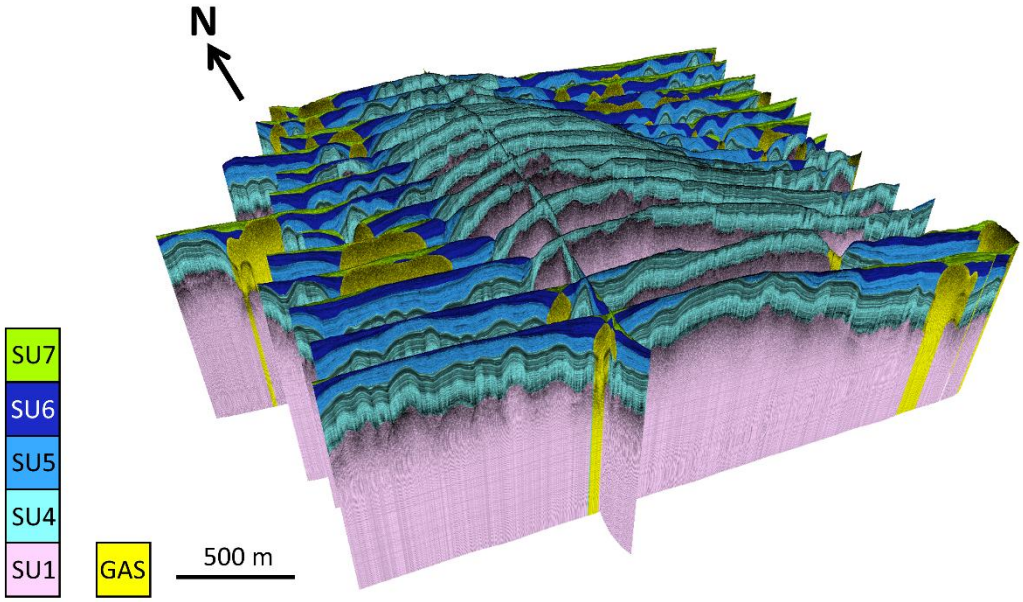

Figure 35. Three-dimensional visualisation of interpreted seismoacoustic units (SU1, SU4–SU7) and gas-related acoustic disturbances in organic-rich sediments (GAS) in study area 4 (Mohni), based on chirp sub-bottom profiles.

The subsurface structure is dominated by a prominent ridge-like feature corresponding to the landform described in the geomorphology section. Within the ridge, the crystalline basement (SU1) is overlain by SU2 and SU3, but the upper glaciolacustrine clay unit (SU4) shows localised erosion and is disrupted by pockmarks. In surrounding deeper areas, the sediment succession thickens and includes a more complete sequence of glaciolacustrine and postglacial sediments (SU4–SU7). Gas-related features are concentrated in these deeper areas.

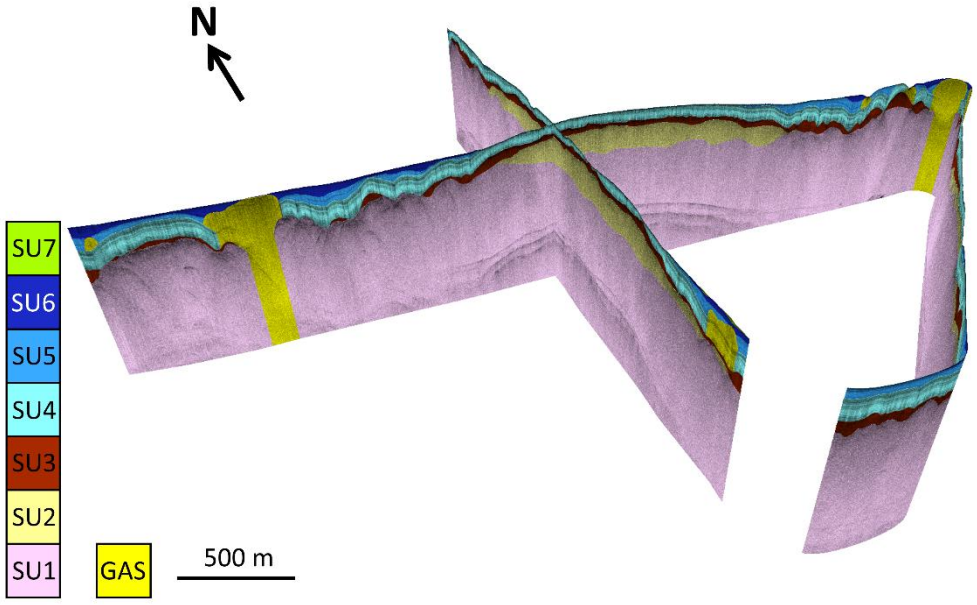

Figure 36. Three-dimensional visualisation of interpreted seismoacoustic units (SU1–SU7) and gas-related acoustic disturbances in organic-rich sediments (GAS) in study area 4 (Mohni), based on boomer seismic profiles.

A representative seismic profile crossing the ridge crest was selected for interpretation (Figure 37). The profile intersects several mapped pockmarks and the main Fe–Mn concretion occurrence zone. Sediment core GOF25-6, collected during the R/V *Electra* 2025 expedition using a gravity coring system, was recovered directly along the same profile line, allowing comparison between the seismic interpretation and lithological data.

Figure 38 presents the representative boomer profile with uninterpreted and interpreted sections. The profile crosses the crest of the ridge-like feature, where three pockmarks intersect the profile line. The inferred Fe–Mn concretion occurrence zone coincides with the ridge crest. The profile clearly resolves the thicker older units (SU2–SU3) beneath the ridge, whereas the upper varved clay unit (SU4) appears thin and discontinuous. In the surrounding deeper areas, the sedimentary succession thickens and includes younger postglacial units (SU5–SU7) together with gas-related features. Multiple reflections within SU1 are interpreted as acoustic artefacts.

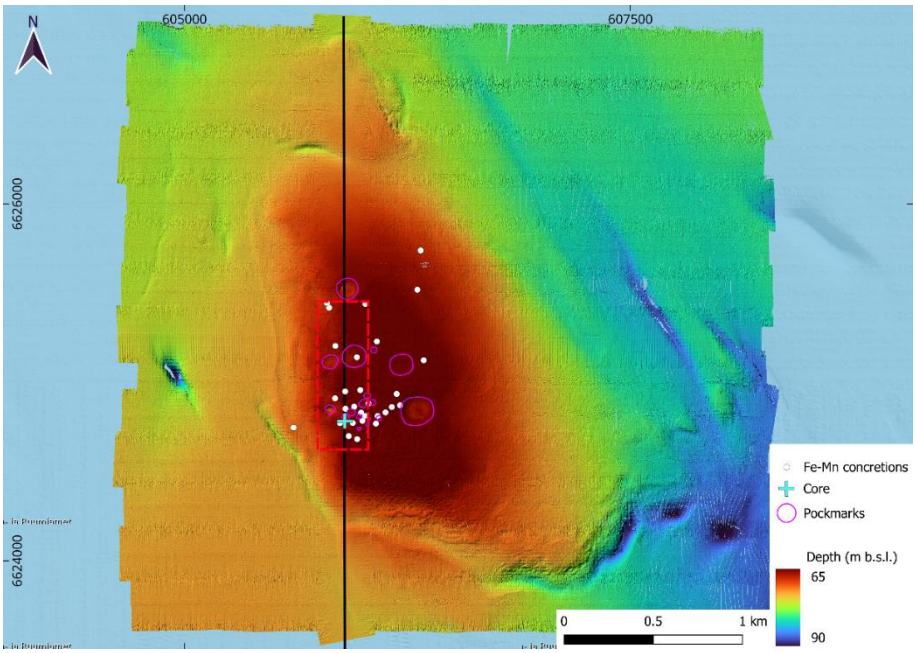

Figure 37. Location of the representative seismoacoustic profile and sediment core GOF25-6 in study area 4 (Mohni), showing mapped pockmarks, Fe–Mn concretion occurrence sites, and the inferred concretion occurrence zone (red dashed box).

The core was recovered from within a pockmark on the ridge crest, where the upper glaciolacustrine clay layer (SU4) is relatively thin. The gravity corer penetrated through SU4 into the underlying glacigenic unit SU3. The core's lithological descriptions, provided by the Geological Survey of Estonia (Sten Suuroja), show good agreement with the seismic interpretation.

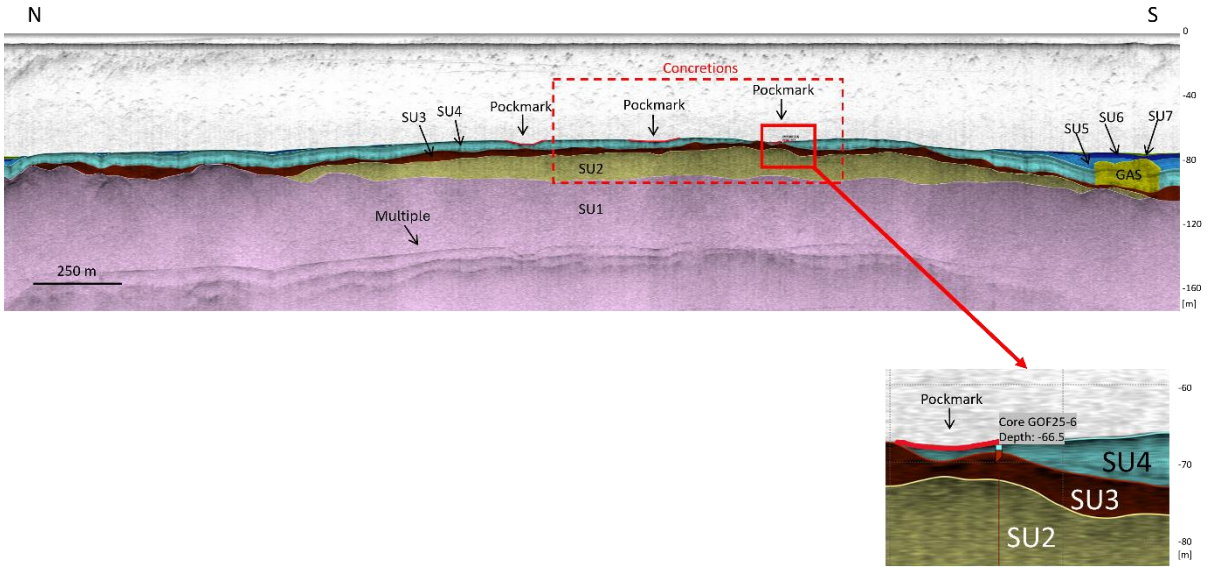

Figure 38. Boomer seismic profile from study area 4 (Mohni) showing interpreted seismoacoustic units (SU1–SU7), an inferred Fe–Mn concretion occurrence zone (red dashed box), and gas-related acoustic disturbances in organic-rich sediments (GAS). The inset shows sediment core GOF25-6 with corresponding stratigraphic boundaries.

6. Discussion

This chapter discusses the main results of the study and interprets the distribution of Fe–Mn concretions in relation to seabed geomorphology, seismostratigraphy, and pockmarks. A total of seven seismoacoustic units (SU1–SU7) were identified across the study areas, but their distribution and preservation vary considerably between study areas. Study area 1 contains the most complete sedimentary succession, whereas study areas 2 and 3 have a reduced set of units. In study area 4, some of the deeper units could only be resolved in the boomer data due to the limited penetration depth of the chirp profiles. The occurrence of seismoacoustic units features is summarised in Table 2.

Table 2. Identified seismoacoustic units in the four study areas.

Study area/ seismoacoustic unit	1	2	3	4
SU7	x	x	x	x
SU6	x		x	x
SU5	x		x	x
SU4	x	x	x	x
SU3	x	x	x	x
SU2	x			x
SU1	x	x	x	x

Although the units were identified based on their acoustic character, geometry, and stratigraphic position, units with the same label do not necessarily represent identical stratigraphic units in all study areas. Due to limited sediment core coverage and the absence of direct lithological control for some units, correlations between areas should therefore be regarded as tentative.

6.1. Geological Interpretation of the Seismoacoustic Units

SU1 forms the deepest and most laterally continuous seismoacoustic unit in all study areas and can be followed across all seismic profiles. SU1 is interpreted as the crystalline basement, although no direct lithological confirmation is available. Its strong and continuous acoustic character suggests that it represents a regional geological boundary underlying the sedimentary bedrock and Quaternary cover. In several locations, particularly on elevated ridge-like features, SU1 occurs very close to the seabed or is locally exposed due to erosion and reduced sediment accumulation. This is especially evident in study area 3, where upper sediment units are thin or absent. The shallow depth of SU1 on elevated seabed features indicates that these areas have likely experienced prolonged sediment starvation and erosional reworking. The close association between exposed or shallow SU1, pockmarks, and Fe–Mn concretions further suggests that basement seabed topography may influence bottom currents, sediment distribution, and fluid migration pathways within the study areas.

SU2 is a local seismoacoustic unit identified only within the ridge-like features of study areas 1 and 4. Its geological interpretation remains uncertain because direct lithological control is limited. Based on its stratigraphic position beneath SU3, SU2 may represent either sedimentary bedrock or older Quaternary deposits. One possible interpretation is that SU2 corresponds to Ediacaran sedimentary bedrock underlying the Quaternary succession in the Gulf of Finland (Kitterød et al., 2022). Regional geological maps place the study areas close to the northern boundary of a mapped Ediacaran outcrop zone (Vallius et al., 2022), supporting the possibility that SU2 may locally represent Ediacaran sandstone or siltstone forming the core of the ridge-like features. The restriction of SU2 to elevated ridge structures is also consistent with a more resistant bedrock unit underlying the Quaternary sediments. However, the offshore bedrock maps in the Gulf of Finland are uncertain, and the interpretation remains tentative without direct lithological evidence.

Alternative interpretations include older Quaternary deposits, such as Eemian interglacial sediments (Miettinen et al., 2002, 2014), which have previously been identified on islands in the Gulf of Finland (Kiipli et al., 1993). Another possibility is that SU2 represents Early or Middle Weichselian deposits, including equivalents of the Voka Middle Weichselian interstadial sediments from northeastern Estonia (Molodkov et al., 2007). The only physical sediment evidence potentially linked to SU2 derives from the *EVA-316* expedition in 2023. The sediment sample (Figure 39) was collected using an ROV manipulator arm from the slope of a mega-scale drumlin at the raised rim of a pockmark (Figures 40 and 41). A nearby W–E-oriented boomer profile, located approximately 250 m north of the sampling site, shows SU2 occurring close to the seabed along the edge of the same ridge-like feature. However, because the sampling location does not lie directly on a seismic profile and the geometry of SU2 is laterally variable, the exact stratigraphic origin of the sample remains uncertain.

Figure 39. Sample GOF23-7 collected from the side of a ridge-like seabed feature in study area 1 during the 2023 *EVA-316* expedition. Based on nearby seismic interpretation, the sample may possibly represent SU2. *Photo by Gennadi Baranov.*

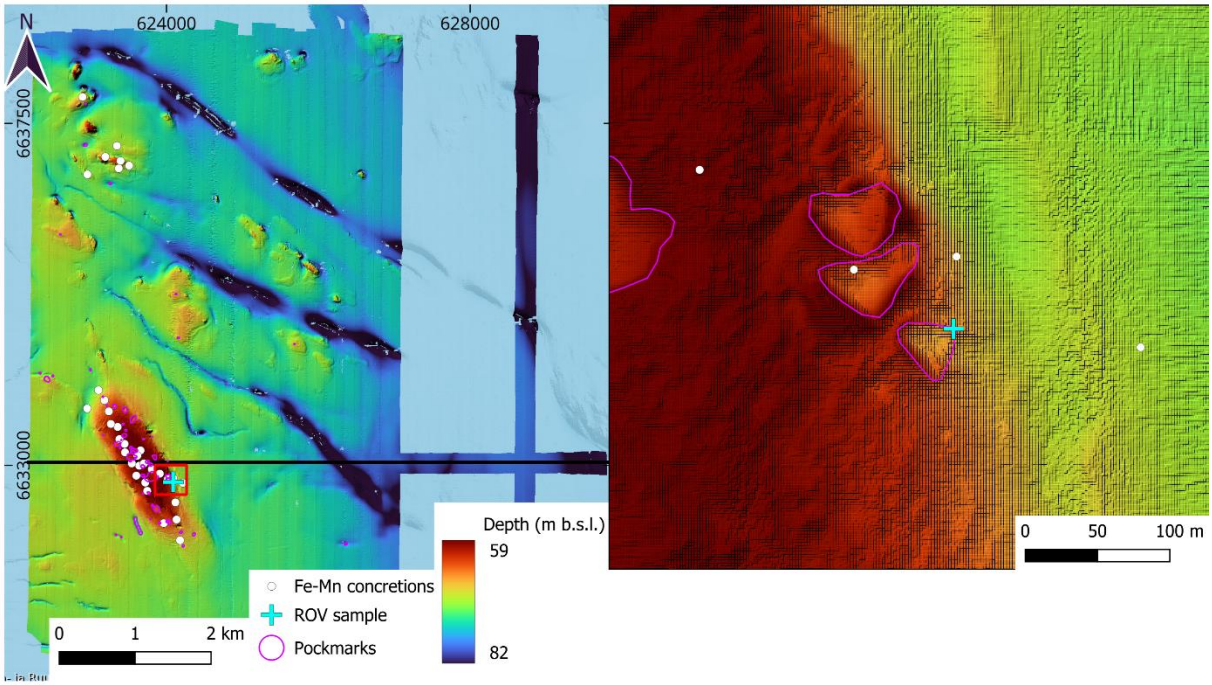

Figure 40. Bathymetric map of study area 1 (Vaindloo West) showing the location of the ROV-collected sample GOF23-7, Fe–Mn concretion occurrences, and the nearest seismoacoustic profile track. The inset shows a detailed view of the sampling location.

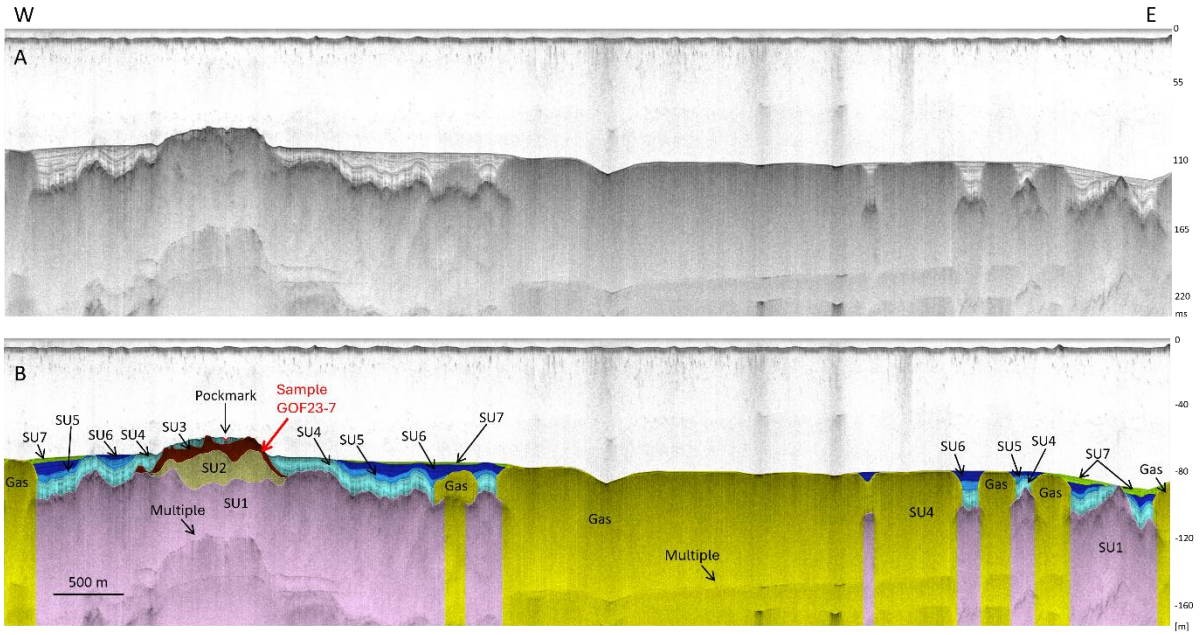

Figure 41. Closest boomer seismic profile to sampling site GOF23-7 in the study area 1 (Vaindloo West): (a) uninterpreted and (b) interpreted profile showing seismoacoustic units (SU1–SU7), gas-related features, pockmarks, and gas-related acoustic disturbances in organic-rich sediments (GAS). The tentative position of sediment sample GOF23-7 is indicated on the profile.

The sample was analysed using several sedimentological and biostratigraphical methods. Pollen analysis was carried out by Siim Veski and diatom analysis by Atko Heinsalu. In addition, loss-on-ignition analysis at 550°C, grain-size analysis (Merlin Liiv), and X-ray fluorescence analysis (Nata-Ly Pantšenko) were performed. The sediment showed elevated organic matter content (5.8–6.5%). XRF results indicate relatively high SiO_2 (53.4%) and Al_2O_3 (14.6%) contents together with elevated Fe_2O_3 (10.9%) and MnO (0.7%). Grain-size analysis revealed a dominant fine-silt fraction, poor sorting, and a fine-skewed distribution, suggesting deposition in a low-energy basin environment affected by episodic higher-energy inflow or resuspension events.

The pollen assemblage includes pine, birch, spruce, herbaceous plants, as well as *Lycopodium* and *Pteridium* spores. These data exclude an Ediacaran age and instead indicate a Quaternary origin. The relatively high abundance and generally good preservation of pollen grains further suggest that the sediment does not represent glacial till. Although diatoms were absent, the sample contained abundant *Pediastrum* green algae, indicating deposition in a freshwater environment. Based on the pollen assemblage (Siim Veski, pers. comm., 2023), the sediment most likely represents Middle Weichselian interstadial deposits comparable to those described from the Voka section in northeastern Estonia (Molodkov et al., 2007). Therefore, the available sedimentological and palaeoecological evidence favours a Quaternary interpretation for the sampled material rather than an Ediacaran bedrock origin. However, because the exact stratigraphic relationship between the sample and SU2 remains uncertain, the possibility that SU2 locally represents sedimentary bedrock beneath the ridge-like features cannot be excluded.

The interpretation of SU3 is confirmed by direct lithological evidence from study area 4. Core GOF25-6, collected during the R/V *Electra* expedition in 2025, penetrated through approximately 80 cm of glaciolacustrine varved clay (SU4) into about 20 cm of underlying till assigned to SU3 (Figure 42). The core was recovered from the crest of a ridge-like feature interpreted as a mega-scale drumlin. The geometry of SU3 is also consistent with glacigenic deposition. In elevated areas, the unit commonly forms thin and discontinuous layers or occurs directly beneath erosional surfaces, whereas in depressions it locally thickens and infills irregularities in the underlying surface. Such variability is characteristic of subglacial till and related glacigenic sediments deposited under dynamic ice-sheet conditions (Evans et al., 2006). The stratigraphic position of SU3 beneath Baltic Ice Lake varved clay (SU4), together with its widespread occurrence across all study areas, further supports its interpretation as Late Weichselian till deposited beneath the Fennoscandian Ice Sheet.

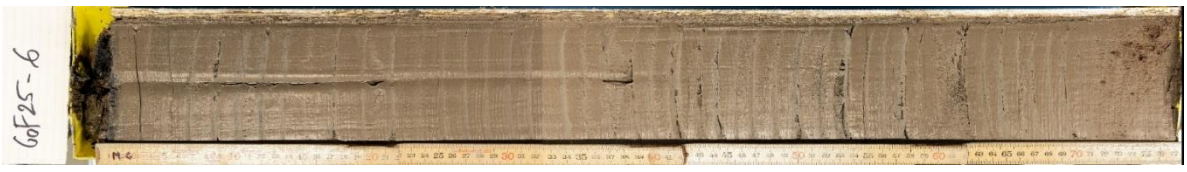

Figure 42. Photograph of gravity core GOF25-6 from study area 4 (Mohni), collected within the project *Security and Management of Coastal Groundwater Resources and Marine Ecosystem Services* (SECUCOAST – MOB3PRT9). The core consists of approximately 80 cm of varved clay overlying 20 cm of till recovered in the core catcher of the R/V *Electra* gravity coring system. Coordinates (ETRS89/L-EST97): 6624783.15 N, 605898.90 E. *Photo by Sten Suuroja.*

SU4 is present in all study areas as a laterally continuous unit that is typically around 10 m thick. It conformably drapes the underlying topography. Its acoustic character, geometry, and correlation with sediment cores (e.g. M_87_018006, M_86_051010, M_87_020002, and GOF25-6) support its interpretation as glaciolacustrine varved clay deposited during the Baltic Ice Lake stage. This interpretation is consistent with previous descriptions of Baltic Ice Lake deposits in the Gulf of Finland (Winterhalter, 1992).

The Baltic Ice Lake formed as a large meltwater basin dammed against the retreating Fennoscandian Ice Sheet during the Late Weichselian deglaciation. Seasonal meltwater input from the retreating ice margin produced annually laminated sediments (varves) consisting of alternating silt-rich and clay-rich layers. In the Gulf of Finland, these varved clays commonly form thick sedimentary sequences, often reaching approximately 10 m in thickness, and therefore represent one of the most regionally extensive and acoustically distinctive stratigraphic units in the shallow subsurface (Lutt & Raukas, 1993). Their widespread occurrence and relatively uniform acoustic character make SU4 an important regional marker horizon for interpreting the postglacial geological development of the Gulf of Finland.

The thickness and continuity of SU4 also indicate that glaciolacustrine sedimentation during the Baltic Ice Lake stage was one of the major depositional phases controlling the present-day sediment stratigraphy of the study areas. In elevated seabed areas, SU4 is commonly thin, eroded, or partly absent, whereas thicker and more continuous successions are preserved in surrounding depressions. This distribution reflects the combined effects of original depositional topography and subsequent postglacial erosion and sediment redistribution.

SU5 is interpreted as a postglacial unit present in study areas 1, 3, and 4 but absent from study area 2. Its absence in area 2 agrees with earlier studies showing that postglacial sediments are limited at the seafloor in this part of the eastern Gulf of Finland (Suuroja et al., 2016). Where present, SU5 mainly occurs in deeper areas surrounding the elevated seabed features, which is consistent with deposition in lower-energy environments characterised by enhanced sediment accumulation.

Based on its stratigraphic position above the Baltic Ice Lake varved clay unit (SU4) and below younger postglacial sediments (SU6–SU7), SU5 is interpreted as a fine-grained postglacial sediment deposited during the Yoldia Sea and Ancylus Lake stages. This interpretation is supported by the R/V *Marina* sediment cores M_87_018006 and M_87_020002.

Yoldia Sea and Ancylus Lake sediments in the Gulf of Finland are typically composed of homogeneous or weakly laminated fine-grained silty clay and clay (Lepland et al., 1999; Heinsalu et al., 2000; Winterhalter, 1992). Acoustically, these deposits are difficult to distinguish from each other because both units generally display relatively uniform internal acoustic character and weak reflector patterns compared to the underlying varved clays of the Baltic Ice Lake stage. For this reason, they are interpreted together as a single seismoacoustic unit (SU5). The distribution of SU5 also reflects the postglacial palaeoenvironmental development of the Gulf of Finland. During the Yoldia Sea and Ancylus Lake stages, sedimentation mainly occurred in deeper and more protected basin areas, whereas elevated seabed features were more strongly affected by erosion and reduced sediment accumulation.

SU6 shows a distribution pattern similar to SU5 and is also absent in study area 2. It mainly occurs in deeper areas between elevated seabed features, where it locally forms a relatively thick and acoustically well-defined unit. This distribution suggests preferential accumulation of fine-grained sediments in deeper and more sheltered basin environments. The interpretation of SU6 is supported by R/V *Marina* sediment core data from study areas 1 and 3.

Based on its stratigraphic position above SU5 and the available sediment core data, SU6 is interpreted as postglacial mud, corresponding to Litorina Sea deposits. Litorina Sea sediments in the Gulf of Finland are typically composed of fine-grained clay and organic-rich mud deposited under brackish-water conditions (Andrén et al., 2011). Their higher organic matter content and laminated character distinguish them from the older Yoldia Sea and Ancylus Lake deposits. The internal structure of SU6 likely reflects changing bottom-water oxygen conditions during the Litorina Sea stage. Under anoxic conditions, fine micro-laminated sediments accumulated due to the absence of benthic bioturbation, whereas periods of improved ventilation and oxygenation promoted benthic activity and the formation of bioturbated muds (Winterhalter, 1992). These alternating environmental conditions may explain some of the internal acoustic variability observed within SU6.

The restriction of SU6 mainly to deeper basin areas also reflects the palaeoenvironmental conditions of the Litorina Sea stage. Elevated seabed features were likely affected by stronger bottom currents, sediment erosion, or reduced sediment accumulation, whereas finer organic-rich mud preferentially accumulated in deeper and more sheltered depressions. The close spatial association between SU6 and gas-related acoustic disturbances further suggests that these organic-rich sediments may act as important gas-generating and gas-retaining layers within the shallow subsurface.

SU7 is the uppermost seismoacoustic unit and occurs in all study areas as a thin, often discontinuous layer. In study areas 1, 3, and 4, SU7 typically overlies SU6, whereas in study area 2 it directly overlies SU4 due to the absence of intermediate units. Based on its stratigraphic position and acoustic character, SU7 is interpreted as the youngest sediment unit and likely corresponds to Limnea Sea muds or locally reworked sandy material. The discontinuous distribution of SU7 suggests that recent sediment accumulation in the study areas has been limited and strongly influenced by erosion and bottom-current activity.

6.2. Controls on Distribution of Iron–Manganese Concretions and Pockmarks

The four study areas show clear differences in seabed geomorphology, sediment structure, and gas occurrence, and these differences appear to strongly influence the distribution of Fe–Mn concretions and pockmarks. Despite local variability, a consistent regional pattern can be recognised: Fe–Mn concretions and pockmarks are preferentially associated with elevated seabed features where sediment cover is thin or locally absent. This relationship is especially evident in study areas 1 and 4 (Vaindloo West and Mohni), where concretions and pockmarks are concentrated on large ridge-like features interpreted as mega-scale drumlins aligned with the regional northwest–southeast glacial landform orientation of the Gulf of Finland (Suuroja et al., 2016).

The distribution of concretions appears closely linked to the relationship between geomorphology and sediment stratigraphy. On elevated seabed features, the glaciolacustrine varved clay unit (SU4) is commonly thin, discontinuous, or partly eroded, while younger postglacial units are largely absent. Consequently, older units such as SU2 and SU3 occur close to the seabed. These areas therefore represent sediment-starved environments. In contrast, surrounding deeper depressions commonly contain thicker postglacial sediment sequences together with more frequent gas-related acoustic disturbances.

This relationship suggests that Fe–Mn concretions preferentially occur in areas where erosion and limited sedimentation maintain oxic conditions at the sediment–water interface. Stronger bottom-current activity on elevated seabed features may prevent the accumulation of fine-grained sediments and help preserve exposed concretion-bearing surfaces. Conversely, thicker postglacial mud accumulations in deeper basin areas bury concretions or create reducing conditions unfavourable for their preservation. The observed distribution of concretions may therefore reflect not only formation processes but also preservation potential.

Study areas 2 and 3 differ from study areas 1 and 4 in that they lack a single dominant ridge structure. Instead, they are characterised by smaller elevated seabed features and rougher local geomorphology, although the regional northwest–southeast alignment is still preserved. In both areas, concretions and pockmarks are concentrated around local topographic highs where older sedimentary units or basement occur close to the seabed. Pockmarks are generally smaller and more circular than those observed in study areas 1 and 4, and many contain small central elevations that may reflect localised sediment redistribution, residual erosional remnants, or focused seepage conduits.

The morphology of the pockmarks also differs between the study areas. In study area 1, pockmarks are commonly irregular, elongated, or partly merged, which may indicate repeated or spatially focused seepage activity. Some pockmarks exhibit raised rims that may have formed through repeated seepage and progressive outward expansion of the depression, resulting in collapse and accumulation of sediment along the margins. In contrast, pockmarks in study area 4 are generally more circular or oval and often contain small central mounds. Larger pockmarks in this area tend to be broader and smoother, which may indicate that they are older or currently less active.

An alternative explanation for some of the large circular depressions observed on ridge crests is that they may represent kettle holes formed by melting of buried ice blocks (Ryabchuk et al., 2020). Kettle holes typically form when detached blocks of glacial ice become buried within glacial sediments and later melt, leaving depressions in the sediment surface (Maizels, 1977). However, the morphology and stratigraphic position of the depressions identified in this study do not fully support a kettle hole origin. The depressions are developed within the glaciolacustrine varved clay unit (SU4) rather than within underlying till units, indicating that they formed after deposition of the varved clays. In addition, a purely glacial origin does not explain their frequent association with Fe–Mn concretions, microbial mats, and other seep-related features.

White microbial mats commonly occur inside the pockmarks and within adjacent concretion fields. This consistent association suggests that fluid seepage from underlying strata plays an important role, and that microbial activity indicates that chemically reduced fluids and microbially mediated redox

processes may contribute to the formation and spatial distribution of Fe–Mn concretions in these environments (Liira et al., 2024). The frequent co-occurrence of pockmarks, Fe–Mn concretions, and microbial mats further supports the interpretation that fluid seepage influences concretion-bearing environments. Elevated seabed features may act as preferential pathways for focused fluid escape. This is because fluids migrating beneath the relatively low-permeability varved clay unit can more easily reach the seafloor at topographic highs. ROV observations from all study areas revealed microbial mats within several concretion-bearing pockmarks (Figure 43). Although direct evidence for submarine groundwater discharge remains limited, the observed spatial associations suggest that localised fluid seepage contributes to redox-controlled mineral precipitation and dissolution processes at the seafloor (Kanapatskiy et al., 2021; Ivanova et al., 2011). Microbially mediated redox reactions may therefore play an important role in the formation and preservation of Fe–Mn concretions in the Gulf of Finland.

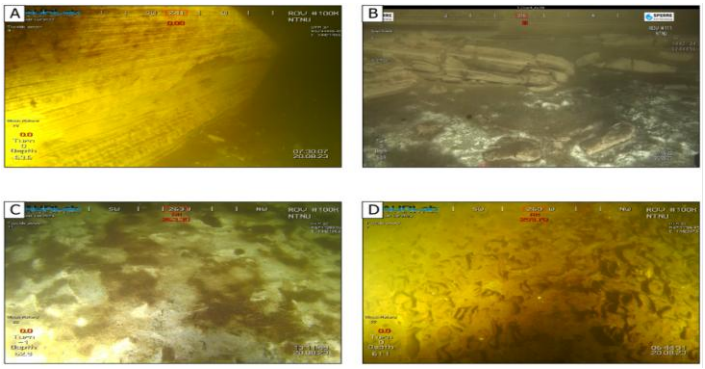

Figure 43. ROV screenshots from the 2023 vessel *EVA-316* expedition illustrating a typical pockmark structure in study area 4 (Mohni): (A) steep pockmark wall composed of glaciolacustrine varved clay; (B) collapsed varved clay blocks and white microbial mats at the base of the pockmark wall; (C) microbial mats covering the floor of the pockmark; and (D) Fe–Mn concretions exposed on the varved clay ridge between neighbouring pockmarks (modified from Mikenberg, 2024).

Gas-related acoustic disturbances are concentrated mainly in study areas 1, 3, and 4, where they are associated with thicker postglacial sediment accumulations in deeper depressions. These organic-rich sediments likely act as gas-generating and gas-retaining layers. The observed gas is most likely methane, which is widespread in Baltic Sea sediments and commonly associated with organic-rich postglacial mud deposits (Schmale et al., 2010). Although fluid migration likely contributes to pockmark formation and concretion-related redox processes, the shallow gas accumulations observed in seismic profiles appear to be mainly associated with organic-rich postglacial sediments in deeper basin areas rather than directly with the concretion-bearing sites themselves. Fluid migration associated with pockmark formation may preferentially occur along erosional surfaces or lithological boundaries between seismoacoustic units, particularly where sediment cover is thin. However, active gas accumulations are not always directly visible beneath individual pockmarks in the seismic profiles, which may indicate episodic seepage activity that does not produce persistent acoustic gas signatures.

Bottom currents likely also contribute to the formation and preservation of concretion-bearing environments. Elongated furrows and trench-like depressions around the ridge structures indicate active or former bottom-current activity. On elevated seabed features, stronger current velocities may

erode fine-grained sediments while leaving heavier Fe–Mn concretions exposed at the seabed. Similar relationships between elevated seabed geomorphology, bottom-current activity, and Fe–Mn mineralisation are known from deep-ocean environments, where ferromanganese crusts commonly occur on sediment-starved seamounts and ridges swept clean by persistent bottom currents (Hein, 2004). Long-term observations from the Gulf of Finland also show that near-bottom currents occur even at water depths greater than 40 m and that storm events can significantly enhance sediment resuspension and transport (Liblik et al., 2013; Rasmus et al., 2015).

Overall, the results indicate that the distribution of Fe–Mn concretions and pockmarks is controlled by a combination of seabed geomorphology, sediment stratigraphy, bottom-current activity, and fluid seepage. Elevated seabed features where older units occur close to the seabed provide favourable conditions for erosion, focused fluid flow, redox cycling, and concretion preservation, whereas surrounding depressions are characterised by thicker postglacial sediment accumulation and more frequent gas-related acoustic disturbances.

6.3. Conceptual Model of Iron–Manganese Concretion Formation

An earlier interpretation linked Fe–Mn concretions in the eastern Gulf of Finland to Ediacaran siliciclastic rocks and a regionally connected groundwater system beneath the Quaternary cover. This interpretation was based on apparent spatial overlap between extensive Fe–Mn concretion fields (Zhamoida et al., 2017) and a broad Ediacaran outcrop belt mapped in the eastern Gulf of Finland (Vallius et al., 2022). A conceptual model proposed in the author's bachelor's thesis (Mikenberg, 2024) suggested that upward migration of groundwater from the Ediacaran sandstone aquifer could contribute to fluid seepage, pockmark formation, and Fe–Mn concretion development in study area 4 (Mohni) (Figure 44).

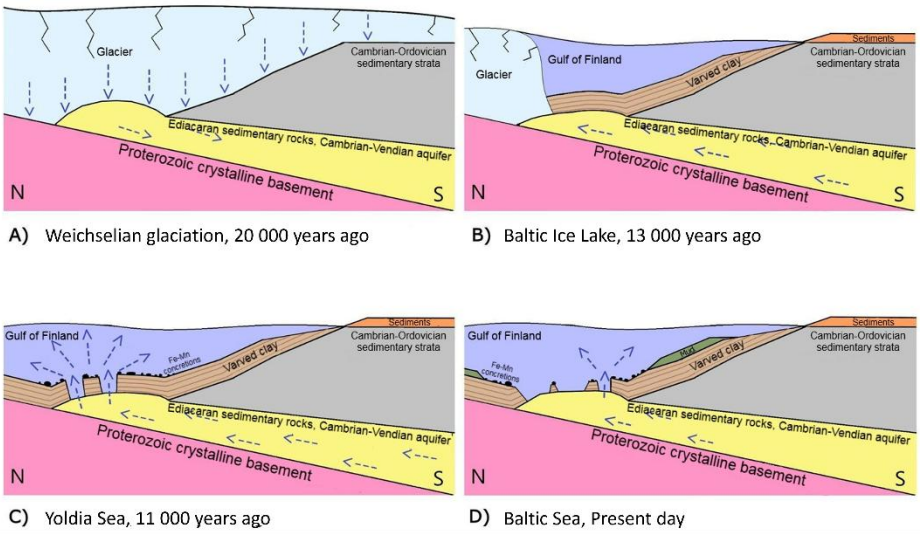

Figure 44. Earlier conceptual model of Fe–Mn concretion formation and fluid migration in the Gulf of Finland proposed by Mikenberg (2024). (A) During the Weichselian glaciation, meltwater infiltrated

deep aquifer systems beneath the Fennoscandian Ice Sheet and transported methane-rich fluids formed within subglacial and periglacial environments. Groundwater flow was directed mainly southward beneath the ice sheet. (B) During the Baltic Ice Lake stage, glaciolacustrine varved clays accumulated while groundwater migrated beneath these low-permeability sediments. During deglaciation and postglacial isostatic rebound, regional groundwater flow likely gradually reversed towards the north. (C) Methane-rich fluids migrated upward towards the seafloor, promoting pockmark formation and Fe–Mn concretion growth. (D) At present day, localised seepage and fluid migration continue along subsurface pathways beneath the Gulf of Finland.

The occurrence of microbial mats within and around concretion-bearing pockmarks suggests that reduced methane-rich fluids are actively or episodically escaping at the seafloor (Liira et al., 2024). Similar seepage-related pockmarks have previously been described from the eastern Gulf of Finland and linked to methane release or submarine groundwater discharge (Ryabchuk et al., 2020). In marine sediments, microbial mats commonly form where upward-migrating methane interacts with sulphate-rich seawater through microbially mediated oxidation processes (Kanapatskiy et al., 2021).

However, the results of the present study suggest that the subsurface system controlling fluid migration and concretion formation is more complex than previously assumed. Fe–Mn concretions are not restricted to areas associated with Ediacaran sedimentary rocks but also occur in regions where Quaternary sediments directly overlie crystalline basement. The seismic interpretation further indicates considerable variability in subsurface structure between concretion-bearing areas. In some locations, glaciolacustrine varved clays overlie glacial till and localised older sedimentary units, whereas in other areas, the Quaternary succession rests directly on crystalline basement.

Although SU2 may locally represent Ediacaran sedimentary rocks within ridge-like features in study areas 1 and 4, these occurrences appear discontinuous rather than forming a laterally extensive regional aquifer system. In the eastern Gulf of Finland, extensive Fe–Mn concretion fields commonly occur within the broad Ediacaran outcrop belt mapped by Vallius et al. (2022). However, concretion-bearing areas are also known from parts of the Gulf of Finland where Quaternary sediments are interpreted to directly overlie crystalline basement.

The results therefore suggest that, within the investigated areas, fluid migration is controlled by a combination of basement-related fracture systems, weathered basement zones, local sedimentary units, permeability contrasts, and seabed geomorphology rather than by a single continuous aquifer system. Studies from Finland and elsewhere in the Fennoscandian Shield have shown that methane may occur within deep fractured crystalline basement through both abiotic and microbially mediated processes (Kietäväinen & Purkamo, 2015). Fractured basement and weathered basement zones may therefore provide important pathways for methane-rich fluids and groundwater migration beneath the Quaternary cover.

Although Ediacaran siliciclastic deposits may not form a continuous regional aquifer system, their relatively high permeability may still locally enhance lateral fluid migration beneath the low-permeability varved clays. Together with fractured basement zones, glacial till, and possible interstadial deposits, these units may facilitate focused upward migration beneath elevated seabed features (Figure 45).

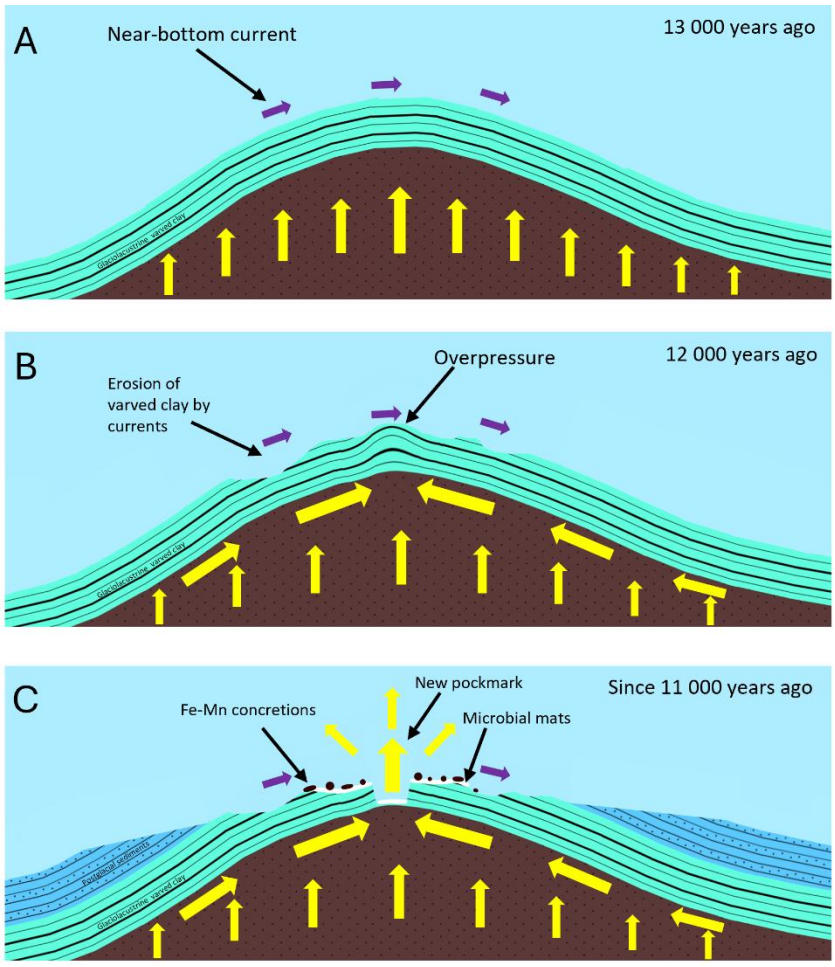

Figure 45. Conceptual model of fluid migration, overpressure development, pockmark formation, and Fe–Mn concretion occurrence. (A) During the Baltic Ice Lake stage (~13 ka), fluids migrate laterally beneath low-permeability glaciolacustrine varved clays towards elevated seabed areas where sediment accumulation is limited. (B) Bottom-current activity began eroding the varved clay cover on topographic highs, while upward fluid migration became increasingly focused beneath ridge-like features, promoting localised overpressure development beneath the varved clay sequence. (C) Since at least the Yoldia Sea stage (~11 ka), release of overpressure through the seabed has allowed methane-rich fluids to escape at the seafloor, forming pockmarks. Localised seepage and redox gradients promote microbial mat development along with the formation, preservation, and exposure of Fe–Mn concretions around seepage structures.

At the seafloor, upward migration of methane-rich fluids likely creates localised redox gradients where reduced pore fluids interact with oxygenated bottom waters. Methane migrating upward through the sediments may also interact with sulphate derived from seawater, promoting microbial methane oxidation and reducing conditions within the sediments. Under such conditions, previously formed iron and manganese oxyhydroxides may dissolve and become mobile. When these dissolved elements later encounter more oxygenated conditions near the sediment surface, they may subsequently reprecipitate as oxyhydroxides and contribute to Fe–Mn concretion growth (Wasiljeff et al., 2025b).

In addition to seepage-related processes, Fe–Mn concretion formation likely also depends on the regional availability of dissolved iron, manganese, and other chemical constituents derived from seawater, riverine input, and sediment remobilisation within the Baltic Sea. Large river systems such as the Neva River may therefore represent important long-term sources of dissolved material to the eastern Gulf of Finland (Zhamoida et al., 2017).

Along with low sedimentation rates and bottom-current erosion of fine-grained sediments, these conditions may promote repeated dissolution and reprecipitation of Fe–Mn oxyhydroxides over long periods. Elevated seabed features may remain exposed for prolonged periods following deglaciation, allowing continued seepage-related redox cycling and long-term concretion growth. The occurrence of microbial mats and seepage-related structures within several pockmarks further suggests that at least some of these processes may remain active today.

7. Conclusions

This thesis investigated the distribution of Fe–Mn concretions in relation to seabed geomorphology, seismostratigraphy, pockmarks, and fluid seepage in four study areas of the Gulf of Finland.

The results show that Fe–Mn concretions are mainly concentrated on elevated seabed features affected by erosion, where sediment cover is thin or absent and older sedimentary units or crystalline basement occur close to the seabed. However, the geological structure of these features differs between the study areas, which indicates that concretion occurrence is not linked to a single geological setting or seismoacoustic unit. Although seven seismoacoustic units (SU1–SU7) were identified, concretions are consistently associated with exposed or near-surface glaciolacustrine varved clays (SU4).

A clear spatial relationship was observed between Fe–Mn concretions and pockmarks in all study areas. The results suggest that elevated seabed features may favour focused fluid migration beneath low-permeability glaciolacustrine varved clays and create suitable conditions for pockmark formation and Fe–Mn concretion preservation. The frequent co-occurrence of pockmarks, concretions, and microbial mats further supports the interpretation that localised fluid seepage and redox-controlled processes influence concretion-bearing environments.

The study indicates that Fe–Mn concretion distribution within the investigated study areas of the Gulf of Finland is controlled by the interaction of seabed geomorphology, sediment stratigraphy, bottom-current activity, erosion, and localised fluid seepage. Fluid migration in the study areas is likely controlled by local geological conditions, including permeability contrasts between sedimentary units, fractured crystalline basement, and the geomorphology of elevated seabed features, rather than by a single regional aquifer system.

Further studies combining geophysical data with sediment geochemistry, porewater analyses, isotopic studies, and additional deep sediment coring would help better constrain fluid origin and the processes controlling Fe–Mn concretion formation in the Gulf of Finland. Particularly important would be deeper sediment coring beneath concretion-bearing areas in order to better understand the geological pathways and sources of fluid migration.

Acknowledgements

I would like to thank my supervisor, Atko Heinsalu, for his support and guidance throughout the thesis process. He dedicated a considerable amount of time to reading, correcting, and improving the manuscript, while continuously providing helpful feedback and ideas. Beyond the thesis itself, thanks to him, I had the opportunity to participate in several marine expeditions and to meet many people in the field of marine geology. His support and good humour made the whole process much easier.

I sincerely thank my co-supervisor, Sten Suuroja from the Geological Survey of Estonia, for his help with the interpretation of the seismoacoustic data and for sharing useful materials, ideas, and practical suggestions throughout this work, and for clarifying the roles of the institutions involved in the study.

I would like to thank Vladimir Karpin for providing the digital terrain models used in this study and for sharing valuable advice related to data processing and interpretation.

I am also grateful to Aivo Lepland for his advice and feedback during the writing process. His ideas and theories played an important role in shaping the hypotheses and discussion of this thesis.

I thank Siim Veski for carrying out the pollen analysis and for his interpretations related to the 2023 sample material. In addition, thanks go to Merlin Liiv for assistance with the loss-on-ignition and grain-size analyses, and Nata-Ly Pantšenko for assistance with the X-ray fluorescence analysis.

Finally, I would like to thank everyone else who participated in the field expeditions, sample collection, and discussions related to this study.

References

Andrén, T., Björck, S., Andrén, E., Conley, D., Zillén, L., & Anjar, J. (2011). The development of the Baltic Sea Basin during the last 130 ka. In J. Harff, S. Björck, & P. Hoth (Eds.), *The Baltic Sea basin* (pp. 75–97). Springer. https://doi.org/10.1007/978-3-642-17220-5_4

Baturin, G. N. (2009). Geochemistry of ferromanganese nodules in the Gulf of Finland, Baltic Sea. *Lithology and Mineral Resources, 44*(5), 411–426. https://doi.org/10.1134/S0024490209050010

Björck, S. (1995). A review of the history of the Baltic Sea, 13.0–8.0 ka BP. *Quaternary International, 27*, 19–40. https://doi.org/10.1016/1040-6182(94)00057-C

Chopra, S., & Marfurt, K. (2023). Pockmarks and their seismic attribute signatures. *AAPG Explorer.* Retrieved August 18, 2025, from https://explorer.aapg.org/story/articleid/65478/pockmarks-and-their-seismic-attribute-signatures

Christ, R. D., & Wernli Sr., R. L. (2014). *The ROV manual: A user guide for remotely operated vehicles* (2nd ed.). Butterworth-Heinemann. https://doi.org/10.1016/C2011-0-07796-7

EMODnet Geology Portal. (n.d.). *Geology* [Map]. Retrieved July 15, 2025, from https://emodnet.ec.europa.eu/en/geology

Estonian Land and Spatial Development Board. (2025a). Coloured relief shading [WMS layer].

Estonian Land and Spatial Development Board. (2025b). Relief shading [WMS layer].

Estonian Research Information System. (2025). *Iron-manganese concretions of the Estonian marine area: distribution, formation mechanisms and economic potential (TEM-TA122)* [Research and development project]. https://www.etis.ee/portal/projects/display/fbbba565-e766-486a-be43-219a7d0951fb

Evans, D. J. A., Phillips, E. R., Hiemstra, J. F., & Auton, C. A. (2006). Subglacial till: Formation, sedimentary characteristics and classification. *Earth-Science Reviews, 78*, 115–176. https://doi.org/10.1016/j.earscirev.2006.04.001

Flodén, T. (1981). Current geophysical methods and data processing techniques for marine geological research in Sweden. *Stockholm Contributions in Geology, 37*, 49–66.

Flodén, T. (2009). *Instructions for online digital processing and interpretation of acoustic and seismic recordings in the Meridata MDPS ver. 5.1 format and their presentation in digital level maps.*

Gibbard, P. L., & Knudsen, K. L. (2025). *Palaeoenvironmental evolution of the Baltic Sea basin during the Last Interglacial (Eemian, Mikulino stages)—a review*. *Boreas*, 55, 282–307. https://doi.org/10.1111/bor.70040

GreenStar Technical Services JSC. (n.d.). *Hydrographic survey* [Web page]. GreenStar Technical Services JSC. Retrieved January 31, 2026, from https://gts.com.vn/our-services/hydrographic-survey/

Hang, T., Veski, S., Vassiljev, J., Poska, A., Kriiska, A., & Heinsalu, A. (2020). A new formal subdivision of the Holocene Series/Epoch in Estonia. *Estonian Journal of Earth Sciences*, *69*, 269–280. https://doi.org/10.3176/earth.2020.15

Harff, J., Björck, S., & Hoth, P. (2011). The Baltic Sea Basin: Introduction. In J. Harff, S. Björck, & P. Hoth (Eds.), *The Baltic Sea basin* (pp. 3–9). Springer. https://doi.org/10.1007/978-3-642-17220-5

Hein, J. R. (2004). Cobalt-rich ferromanganese crusts: Global distribution, composition, origin and research activities. In *Minerals other than polymetallic nodules of the International Seabed Area* (pp. 188–256). Proceedings of a workshop held on 26-30 June 2000. International Seabed Authority.

Hein, J. R., Koschinsky, A., & Kuhn, T. (2020). Deep-ocean polymetallic nodules as a resource for critical materials. *Nature Reviews Earth & Environment, 1,* 158–169. https://doi.org/10.1038/s43017-020-0027-0

Heinsalu, A. (2001). Diatom stratigraphy and the palaeoenvironment of the Yoldia Sea in the Gulf of Finland, Baltic Sea. *Annales Universitatis Turkuensis Series A II Biologica-Geographica-Geologica, 144*, 1–42.

Heinsalu, A., Alliksaar, T., Liiv, M., Kallaste, T., Urtson, K., Karpin, V., Suuroja, S., Tuuling, I., & Veski, A. (2021). *Merepõhja geoloogia: Geofüüsikalised kaugseire meetodid ja setete uuringud*. Tallinna Tehnikaülikool, Geoloogia Instituut; Eesti Geoloogiateenistus. [In Estonian with English summary]. https://sisu.ut.ee/wp-content/uploads/sites/356/2_3_2_seabed_geological_inventories_acoustic_profiling_and_sediment_survey.pdf

Heinsalu, A., Kohonen, T., & Winterhalter, B. (2000). Early post-glacial environmental changes in the western Gulf of Finland based on diatom and lithostratigraphy of sediment core B–51. *Baltica*, *13*, 51–60.

Heinsalu, A., & Veski, S. (2007). The history of the Yoldia Sea in Northern Estonia: palaeoenvironmental conditions and climatic oscillations. *Geological Quarterly*, *51*, 295–306.

Hughes, A. L. C., Gyllencreutz, R., Lohne, Ø. S., Mangerud, J., & Svendsen, J. I. (2016). The last Eurasian ice sheets – A chronological database and time-slice reconstruction, DATED-1. *Boreas, 45*, 1–45. https://doi.org/10.1111/bor.12142

Hydro International. (n.d.). *Sub-bottom object detection*. Hydro International. Retrieved February 2, 2026, from https://www.hydro-international.com/content/article/sub-bottom-object-detection

Hyttinen, O., Kotilainen, A., & Salonen, V.-P. (2011). Acoustic evidence of a Baltic Ice Lake drainage debrite in the northern Baltic Sea. *Marine Geology, 284*, 139–148. https://doi.org/10.1016/j.margeo.2011.03.014

Ivanova, V., Kirievskaya, D., & Bolotov, A. (2011). *The geochemical characteristics of the bottom sediment in the pockmark area of the eastern part of the Gulf of Finland*. *Baltic Region, 3*, 68–78. http://dx.doi.org/10.5922/2079-8555-2011-1-9

Kadastik, E., Kalm, V., Liivrand, E., Mäemets, H., & Sakson, M. (2003). Stratigraphy of a site with Eemian interglacial deposits in north Estonia (Juminda peninsula). *GFF*, *125*, 229–236. https://doi.org/10.1080/11035890301254229

Kanapatskiy, T. A., Ulyanova, M. O., Iasakov, T. R., Shubenkova, O. V., & Pimenov, N. V. (2021). *Microbial processes of carbon and sulfur cycles in sediments of the Russian sector of the Baltic Sea*. In E. E. Ezhova, O. V. Kocheshkova, & A. G. Kostianoy (Eds.), *Marine biota of the southeastern Baltic Sea: Environmental studies in the Kaliningrad region* (pp. 1–39). Springer. https://doi.org/10.1007/698_2021_818

Kietäväinen, R., & Purkamo, L. (2015). The origin, source, and cycling of methane in deep crystalline rock biosphere. *Frontiers in Microbiology, 6*, 725. https://doi.org/10.3389/fmicb.2015.00725

Kiipli, T., Liivrand, E., Lutt, J., Pirrus, R., & Rennel, G. (1993). Pinnakate. In J. Lutt & A. Raukas (Eds.), *Eesti šelfi geoloogia* (pp. 76–103). Eesti Geoloogia Selts; Eesti Teaduste Akadeemia Geoloogia Instituut; Eesti Geoloogiakeskus. [In Estonian]. https://www.etera.ee/s/yyhwhgLLM2

Kitterød, N.-O., Kværner, J., Aagaard, P., Arustienė, J., Bikše, J., Dagestad, A., Gundersen, P., Hansen, B., Hjartarson, Á., Karro, E., Klaviņš, M., Marandi, A., Radienė, R., Retike, I., Rossi, P. M., & Thorling, L. (2022). Hydrogeology and groundwater quality in the Nordic and Baltic countries. *Hydrology Research, 53*, 958–982. https://doi.org/10.2166/nh.2022.018

Lasberg, K. (2012). Weichselian glaciation in Estonia. *Quaternary International, 279–280*, 268. https://doi.org/10.1016/j.quaint.2012.08.673

Lepland, A., Heinsalu, A., & Stevens, R. (1999). The pre-Littorina diatom stratigraphy and sediment sulphidisation record from the west-central Baltic Sea: Implications of the water column salinity variations. *GFF*, *121*, 57–65.

Leppäranta, M., & Myrberg, K. (2009). *Physical oceanography of the Baltic Sea.* Springer. https://doi.org/10.1007/978-3-540-79703-6

Liblik, T., Laanemets, J., Raudsepp, U., Elken, J., & Suhhova, I. (2013). Estuarine circulation reversals and related rapid changes in winter near-bottom oxygen conditions in the Gulf of Finland, Baltic Sea. *Ocean Science*, *9*, 917–930. https://doi.org/10.5194/os-9-917-2013

Liira, M., Ojap, J. M., Lepland, A., Suuroja, S., Ausmeel, M., Szymczycha, B., Hong, W.-L., Böttcher, M. E., Virtasalo, J., Mikenberg, H., Heinsalu, A., & Roopõld, K. (2024). Insights into the genesis and

geological significance of iron–manganese precipitates in the Baltic Sea, Gulf of Finland seafloor. *EGUsphere.* https://doi.org/10.5194/egusphere-egu24-7279

Lurton, X., & Lamarche, G. (Eds.). (2015). *Backscatter measurements by seafloor-mapping sonars: Guidelines and recommendations*. GeoHab Backscatter Working Group.

Lutt, J., & Raukas, A. (Eds.). (1993). *Eesti šelfi geoloogia*. Eesti Geoloogia Selts; Eesti Teaduste Akadeemia Geoloogia Instituut; Eesti Geoloogiakeskus. [In Estonian with English summary]. https://www.etera.ee/s/yyhwhgLLM2

Maizels, J. K. (1977). Experiments on the origin of kettle-holes. *Journal of Glaciology, 18*, 291–303. https://doi.org/10.1017/S0022143000021365

Majamäki, R., Wasiljeff, J., Purkamo, L., Hultman, J., Asmala, E., Yli-Hemminki, P., Jørgensen, K. S., Koho, K., Kuva, J., & Virtasalo, J. J. (2025). Microbially enhanced growth and metal capture by ferromanganese concretions in a laboratory experiment. *Geobiology, 23*. https://doi.org/10.1111/gbi.70010

Menandro, P. S., Misiuk, B., Schneider von Deimling, J., Bastos, A. C., & Brown, C. J. (2025). *Multifrequency seafloor acoustic backscatter as a tool for improved biological and geological assessments: Updating knowledge, prospects, and challenges*. *Frontiers in Remote Sensing, 6*, 1546280. https://doi.org/10.3389/frsen.2025.1546280

Micallef, A., Krastel, S., & Savini, A. (Eds.). (2018). *Submarine geomorphology*. Springer. https://doi.org/10.1007/978-3-319-57852-1

Miettinen, A., Head, M. J., & Knudsen, K. L. (2014). Eemian sea-level highstand in the eastern Baltic Sea linked to long-duration White Sea connection. *Quaternary Science Reviews, 86*, 158–174. https://doi.org/10.1016/j.quascirev.2013.12.009

Miettinen, A., Rinne, K., Haila, H., Hyvärinen, H., Eronen, M., Delusina, I., Kadastik, E., Kalm, V., & Gibbard, P. (2002). The marine Eemian of the Baltic: New pollen and diatom data from Peski, Russia, and Põhja-Uhtju, Estonia. *Journal of Quaternary Science, 17*, 445–458. https://doi.org/10.1002/jqs.706

Mikenberg, H. (2024). *Soome lahe raua-mangaani konkretsioonide tekkemehhanismide seos merepõhja geoloogilise ehituse ja lekkimislehtritega* [Bachelor's thesis, Tallinn University of Technology]. [In Estonian with English summary]. https://digikogu.taltech.ee/et/Item/367ecb5a-ed4a-4e33-9370-f808ae4d76ba

Molodkov, A., Bolikhovskaya, N., Miidel, A., & Ploom, K. (2007). The sedimentary sequence recovered from the Voka outcrops, northeastern Estonia: Implications for late Pleistocene stratigraphy. *Estonian Journal of Earth Sciences, 56*, 47–62.

Nasif, A. (2024). Processing of pinger, Chirp, boomer, and parametric subbottom profiler datasets. *Turkish Journal of Earth Sciences, 33*, 729–745. https://doi.org/10.55730/1300-0985.1941

Ojala, A. E. K., Heinsalu, A., Saarnisto, M., & Tiljander, M. (2005). Annually laminated sediments date the drainage of the Ancylus Lake and early Holocene shoreline displacement in central Finland. *Quaternary International*, *130*, 63–73. https://doi.org/10.1016/j.quaint.2004.04.032

Purkamo, L., Ehlert von Ahn, C. M., Jilbert, T., Muniruzzaman, M., Bange, H. W., Jenner, A.-K., Böttcher, M. E., & Virtasalo, J. J. (2022). Impact of submarine groundwater discharge on biogeochemistry and microbial communities in pockmarks. *Geochimica et Cosmochimica Acta, 334*, 14–44. https://doi.org/10.1016/j.gca.2022.06.040

Rasmus, K., Kiirikki, M., & Lindfors, A. (2015). Long-term field measurements of turbidity and current speed in the Gulf of Finland leading to an estimate of natural resuspension of bottom sediment. *Boreal Environment Research, 20*, 735–747. https://doi.org/10.60910/sbdt-6agn

Rhebergen, F. (2009). Ordovician sponges (Porifera) and other silicifications from Baltica in Neogene and Pleistocene fluvial deposits of the Netherlands and northern Germany. *Estonian Journal of Earth Sciences, 58*, 24–37. https://doi.org/10.3176/earth.2009.1.03

Riikoja, H. (1936). *Järvemaagist ja selle esinemisest Eestis*. *Eesti Loodus*, 89–96. [In Estonian]. https://www.digar.ee/viewer/et/nlib-digar:348119/304450/page/1

Rosentau, A., Bennike, O., Uścinowicz, S., & Miotk-Szpiganowicz, G. (2017). The Baltic Sea. In N. C. Flemming, J. Harff, D. Moura, A. Burgess, & G. N. Bailey (Eds.), *Submerged landscapes of the continental shelf: Quaternary paleoenvironments* (pp. 103–133). Wiley-Blackwell. https://doi.org/10.1002/9781118927823.ch5

Ryabchuk, D., Sergeev, A., Zhamoida, V., Budanov, L., Krek, A., Neevin, I., Bubnova, E., Danchenkov, A., & Kovaleva, O. (2020). High-resolution geological mapping towards an understanding of post-glacial development and Holocene sedimentation processes in the eastern Gulf of Finland: An EMODnet Geology case study. *Geological Society, London, Special Publications, 505*, SP505-2019-127. https://doi.org/10.1144/SP505-2019-127

Schmale, O., Schneider von Deimling, J., Gülzow, W., Nausch, G., Waniek, J. J., & Rehder, G. (2010). Distribution of methane in the water column of the Baltic Sea. *Geophysical Research Letters, 37*, L12604. https://doi.org/10.1029/2010GL043115

SecuCoast. (n.d.). *SecuCoast* [Website]. Retrieved December 8, 2025, from https://secucoast.weebly.com/et.html

Shulga, N., Perfilov, P., & Ryazantsev, K. (2025). *Integrated geochemical and biomarker signature of fast-growing Fe–Mn nodules from the Gulf of Finland, Baltic Sea*. *Frontiers in Marine Science, 12*, 1717972. https://doi.org/10.3389/fmars.2025.1717972

Sternbeck, J., & Sohlenius, G. (1997). Authigenic sulphide and carbonate mineral formation in the Holocene sediments of the Baltic Sea. *Chemical Geology, 135*, 55–73. https://doi.org/10.1016/S0009-2541(96)00104-0

Suuroja, K., All, T., Kõiv, M., Mardim, T., Morgen, E., Ploom, K., & Vahtra, T. (2002). *Eesti geoloogiline baaskaart (mõõtkavas 1:50 000). 7321 Prangli: Seletuskiri*. Eesti Geoloogiakeskus. [In Estonian with English summary].

Suuroja, K., Niin, M., Suuroja, S., Ploom, K., Kaljuläte, K., Talpas, A., & Petersell, V. (2010). *Suur-Pakri saare ja selle lähiümbruse geoloogilis-geotehnilis-hüdrogeoloogiliste uuringute aruanne*. Eesti Geoloogiakeskus. [In Estonian].

Suuroja, S., Heinsalu, A., Tõnisson, H., Lips, U., Lepland, A., Kask, A., Alliksaar, T., Mikomägi, A., Buschmann, F., Petersell, V., Pajusaar, S., Marzecova, A., Erm, A., Nigri, S., Liiv, M., Vandel, E., Milvek, H., Kiipli, T., Orviku, K., … All, T. (2016). *Hinnangu andmine merekeskkonna ökosüsteemipõhiseks korraldamiseks Soome lahe merepõhja ja setete näitel: SedGoF projekti aruanne.* Eesti Geoloogiakeskus. [In Estonian with English summary]. https://kirjandus.geoloogia.info/reference/37368

Szymczycha, B., & Pempkowiak, J. (2016). *The role of submarine groundwater discharge as material source to the Baltic Sea*. Springer. https://doi.org/10.1007/978-3-319-25960-4

Talpas, A., Kivisilla, J., Kõrvel, V., Mardla, A., Petersell, V., Popova, L., Rennel, G., Skitiba, A., Tammik, P., & Fokin, A. (1989). *Soome lahe regionaalne geoloogilis-geofüüsikaline uuring M 1:200 000 kaardilehtedel O-35-II (idaosa), O-35-III, 1986–1989. a* [Regional geological-geophysical investigation of the Gulf of Finland on 1:200,000 map sheets O-35-II (eastern part), O-35-III, 1986–1989] [In Russian]. Eesti Geoloogia, EGF 4339. Geological Survey of Estonia.

Tuit, C. B., & Wait, A. D. (2020). A review of marine sediment sampling methods. *Environmental Forensics, 21*, 291–309. https://doi.org/10.1080/15275922.2020.1771630

Tuuling, I., Bauert, H., Willman, S., & Budd, G. E. (2011). *The Baltic Sea: Geology and geotourism highlights.* GeoGuide Baltoscandia.

Tuuling, I., Suuroja, S., Veski, A., & Liira, M. (2021). *Ülevaade mereliste geoloogiliste andmete kasutamisest meretuuleparkide planeerimisel*. Eesti Geoloogiateenistus. [In Estonian]. https://doi.org/10.23679/1022

Uścinowicz, S. (2014). The Baltic Sea continental shelf. *Geological Society, London, Memoirs, 41*, 69–89. https://doi.org/10.1144/m41.7

Vaknin, I., Aharonov, E., Holtzman, R., & Katz, O. (2024). Gas seepage and pockmark formation from subsurface reservoirs: Insights from table-top experiments. *Journal of Geophysical Research: Solid Earth, 129*, e2023JB028255. https://doi.org/10.1029/2023jb028255

Vallius, H., Alliksaar, T., & Suuroja, S. (2022). Changes in heavy metal concentrations in the sediments of the Gulf of Finland over two decades. *Proceedings of the Estonian Academy of Sciences: Geology, 71*, 177–187. https://doi.org/10.3176/earth.2022.12

Vallius, H., Zhamoida, V., Kotilainen, A., & Ryabchuk, D. (2017). Seafloor desertification – A future scenario for the Gulf of Finland? In N. C. Flemming, J. Harff, D. Moura, A. Burgess, & G. N. Bailey

(Eds.), *Submerged landscapes of the continental shelf: Quaternary paleoenvironments* (pp. 365–372). Springer. https://doi.org/10.1007/978-3-642-17220-5_17

Virtasalo, J. J., Endler, M., Moros, M., Jokinen, S. A., Hämäläinen, J., & Kotilainen, A. T. (2016). Base of brackish-water mud as a key regional stratigraphic marker of mid-Holocene marine flooding of the Baltic Sea Basin. *Geo-Marine Letters, 36*, 445–456. https://doi.org/10.1007/s00367-016-0464-4

Virtasalo, J. J., Hämäläinen, J., & Kotilainen, A. T. (2014a). Toward a standard stratigraphical classification practice for the Baltic Sea sediments: The CUAL approach. *Boreas*, *43*, 924–938. https://doi.org/10.1111/bor.12076

Virtasalo, J. J., Kotilainen, A. T., Räsänen, M. E., & Ojala, A. E. K. (2007). Late-glacial and post-glacial deposition in a large, low relief, epicontinental basin: the northern Baltic Sea. *Sedimentology*, *54*, 1323–1344. https://doi.org/10.1111/j.1365-3091.2007.00883.x

Virtasalo, J. J., Ryabchuk, D., Kotilainen, A. T., Zhamoida, V., Grigoriev, A., Sivkov, V., & Dorokhova, E. (2014b). Middle Holocene to present sedimentary environment in the easternmost Gulf of Finland (Baltic Sea) and the birth of the Neva River. *Marine Geology, 350*, 84–96. https://doi.org/10.1016/j.margeo.2014.02.003

Voronov, A. N., & Viventsova, E. A. (2004). Groundwater runoff into the Gulf of Finland. *Water Resources, 31*, 601–609. https://doi.org/10.1023/b:ware.0000046897.69978.e7

Wasiljeff, J., Lahaye, Y., Lehtonen, A., Fu, R., Salminen, J. M., Michallik, R. M., Kurhila, M., Myllyperkiö, M., & Virtasalo, J. J. (2025a). Centennial to millennial-scale paleoenvironmental record from a coastal iron–manganese concretion. *Communications Earth & Environment*, *6*, 771. https://doi.org/10.1038/s43247-025-02741-z

Wasiljeff, J., Salminen, J. M., Roberts, A. P., Hu, P., Brown, M., Kuva, J., Lukkari, S., Jolis, E. M., Heinsalu, A., Hong, W.-L., Lepland, A., Suuroja, S., Parkkonen, J., & Virtasalo, J. J. (2024). Morphology-dependent magnetic properties in shallow-water ferromanganese concretions. *Geochemistry, Geophysics, Geosystems, 25*, e2023GC011366. https://doi.org/10.1029/2023gc011366

Wasiljeff, J., Yu, C., Heikkilä, P., Lahaye, Y., Kurhila, M., Hong, W.-L., Lepland, A., Suuroja, S., Liebetrau, V., & Virtasalo, J. J. (2025b). Mineral phases and growth conditions of morphologically diverse shelfal ferromanganese concretions. *Geochimica et Cosmochimica Acta, 400*, 227–247. https://doi.org/10.1016/j.gca.2025.05.012

Wheeler, A. (n.d.). Seabed sediment sampling techniques. University College Cork, School of Biological, Earth & Environmental Sciences.

Winterhalter, B. (1992). Late-Quaternary stratigraphy of Baltic Sea basins: A review. *Bulletin of the Geological Society of Finland, 64*, 189–194.

Yanuka-Golub, K., Belkin, N., Weber, N., Mayyani, M., Levy, Y., Reznik, I. J., Rubin-Blum, M., Rahav, E., & Kiro, Y. (2024). Allochthonous groundwater microorganisms affect coastal seawater

microbial abundance, activity, and diversity. *Journal of Geophysical Research: Biogeosciences, 129*, e2023JG007610. https://doi.org/10.1029/2023jg007610

Yli-Hemminki, P., Sara-Aho, T., Jørgensen, K. S., & Lehtoranta, J. (2016). *Iron–manganese concretions contribute to benthic release of phosphorus and arsenic in anoxic conditions in the Baltic Sea*. *Journal of Soils and Sediments, 16*, 2138–2152. https://doi.org/10.1007/s11368-016-1426-1

Zhamoida, V., Grigoriev, A., Gruzdov, K., Ryabchuk, D., Evdokimenko, A., Kotilainen, A. T., Vallius, H., & Kaskela, A. M. (2017). *Ferromanganese concretions of the eastern Gulf of Finland: Environmental role and effects of submarine mining*. *Journal of Marine Systems, 172*, 178–187. https://doi.org/10.1016/j.jmarsys.2017.03.009

Zillén, L., Conley, D. J., Andrén, T., Andrén, E., & Björck, S. (2008). Past occurrences of hypoxia in the Baltic Sea and the role of climate variability, environmental change and human impact. *Earth-Science Reviews*, *91*, 77–92. https://doi.org/10.1016/j.earscirev.2008.10.001

Appendix 1. Chirp trackplots

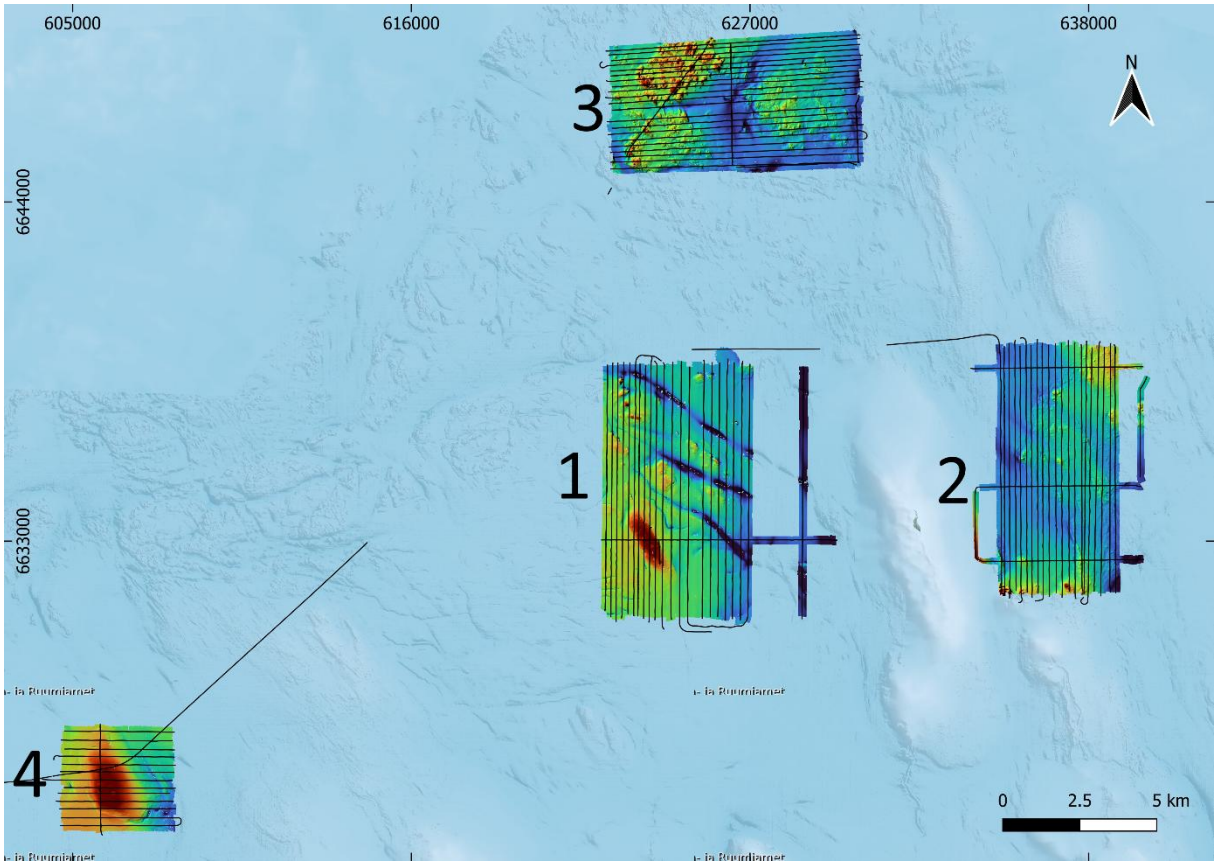

Appendix 2. Boomer trackplots

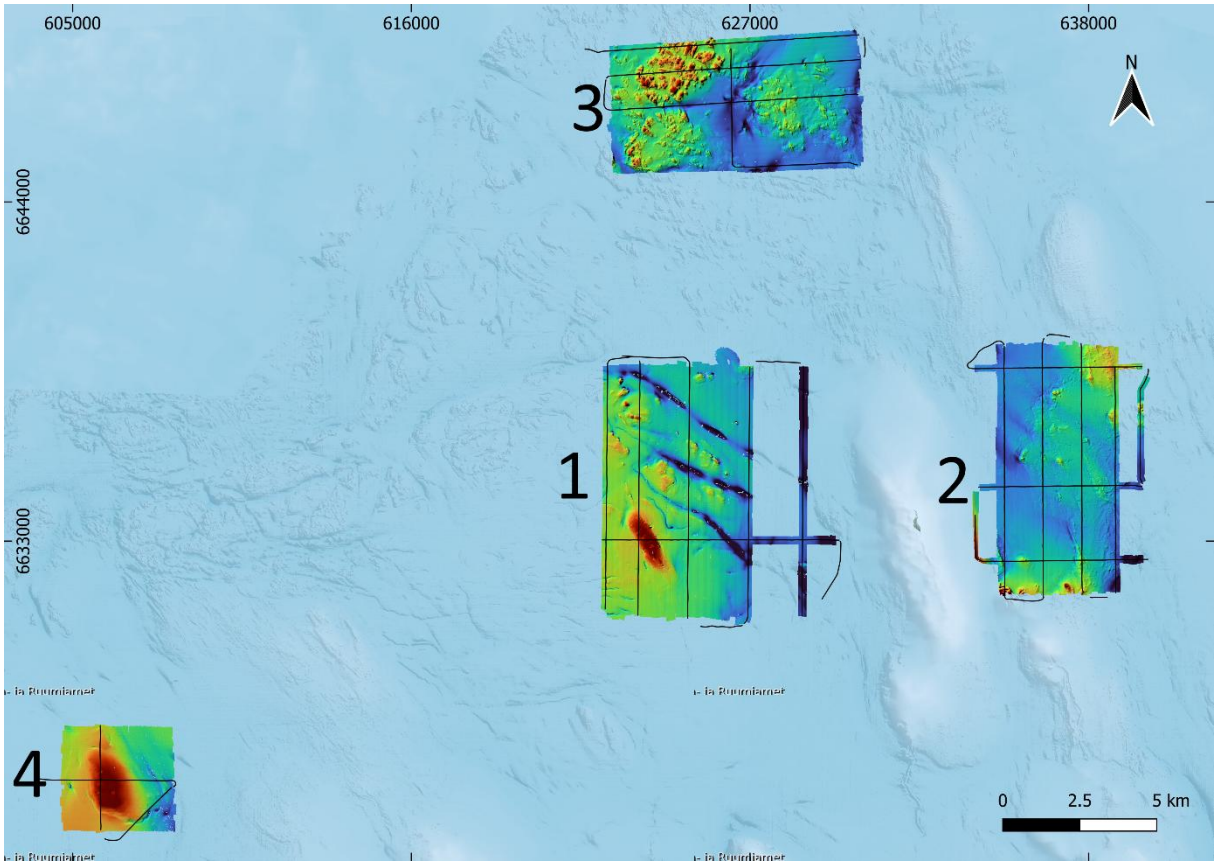

Lisa
rektori 07.04.2020 käskkirjale nr 1-8/17

Lihtlitsents lõputöö reprodutseerimiseks ja lõputöö üldsusele kättesaadavaks tegemiseks[1]

Mina Hannah Mikenberg

1. Annan Tallinna Tehnikaülikoolile tasuta loa (lihtlitsentsi) enda loodud teose "Distribution of iron–manganese concretions in relation to seismostratigraphy in the Gulf of Finland", mille juhendaja on Atko Heinsalu ja kaasjuhendaja Sten Suuroja,

1.1 reprodutseerimiseks lõputöö säilitamise ja elektroonse avaldamise eesmärgil, sh Tallinna Tehnikaülikooli raamatukogu digikogusse lisamise eesmärgil kuni autoriõiguse kehtivuse tähtaja lõppemiseni;

1.2 üldsusele kättesaadavaks tegemiseks Tallinna Tehnikaülikooli veebikeskkonna kaudu, sealhulgas Tallinna Tehnikaülikooli raamatukogu digikogu kaudu kuni autoriõiguse kehtivuse tähtaja lõppemiseni.

2. Olen teadlik, et käesoleva lihtlitsentsi punktis 1 nimetatud õigused jäävad alles ka autorile.

3. Kinnitan, et lihtlitsentsi andmisega ei rikuta teiste isikute intellektuaalomandi ega isikuandmete kaitse seadusest ning muudest õigusaktidest tulenevaid õigusi.

25.05.2026

---

[1] *Lihtlitsents ei kehti juurdepääsupiirangu kehtivuse ajal vastavalt üliõpilase taotlusele lõputööle juurdepääsupiirangu kehtestamiseks, mis on allkirjastatud teaduskonna dekaani poolt, välja arvatud ülikooli õigus lõputööd reprodutseerida üksnes säilitamise eesmärgil. Kui lõputöö on loonud kaks või enam isikut oma ühise loomingulise tegevusega ning lõputöö kaas- või ühisautor(id) ei ole andnud lõputööd kaitsvale üliõpilasele kindlaksmääratud tähtajaks nõusolekut lõputöö reprodutseerimiseks ja avalikustamiseks vastavalt lihtlitsentsi punktidele 1.1. jq 1.2, siis lihtlitsents nimetatud tähtaja jooksul ei kehti.*